DEVELOPMENT OF AN ADAPTIVE THRESHOLD ELEMENT

BY :

PIERRE A. DESCHENES

Submitted in partial fulfillment

of the requirements for the degree of

Master of Science.

Department of Electrical Engineering,

Faculty of Pure and Applied Science,

The University of Ottawa,

Ottawa, Canada.

1963.

ABSTRACT

The present report outlines the progress on the development of an adaptive threshold element. This work is a continuation or an improvement of some electronic nervous cells or neurons that were designed for experiments on adaptability and reliability.

As these experiments dealt with learning, a brief description of the human learning system and of the different types of learning is first introduced. The form of the equipment at the University of Ottawa is then reviewed; the experiments on adaptability and reliability which have been performed using this equipment are then related to the learning process.

The third chapter discusses a few different possibilities for a self-organizing threshold element of the neuron type; a mathematical description of the cell illustrates these various ways. Before the different approaches for our neuron are outlined, some existing hardware models are described. It is then seen that the flux integration seems the most appropriate to realize an adaptive element. The realization is obtained by utilizing a Hall element inserted in the air gap of a square loop ferromagnetic material. This material provides the memory of past activity while the voltage developed by the Hall element is a function of this past activity and varies the threshold of the threshold logic element.

The theory of Hall effect is briefly outlined. It is then shown how a square loop material core can be driven in a number of discrete steps from one saturated state to the opposite one. As an air gap needs to be introduced, its effects are investigated. Ways of minimizing the shearing introduced by the air gap are studied.

The physical realization of the device is then illustrated; some experimental results show that the approach considered is a promising one, even if improvements are still necessary. In the conclusion, the author reviews his work and makes appropriate suggestions as to the amelioration of the functioning of the adaptive threshold logic element.

ACKNOWLEDGMENTS

The author is pleased to express his gratitude and thanks to his project director, Prof. G.S. Glinski; the author is especially grateful for the judicious advices and ideas which have paved the way for the present work.

Chapter 2, as the reader can notice, is a summary of the work of his predecessor, Mr. J. Therrien; the present contribution is only a continuation of Mr. Therrien's long efforts. Much credit should therefore be directed to him.

The author also takes this occasion to thank other members of the Electrical Engineering Department and his fellow graduate students who have shed some light on the problems in the course of discussion.

This research was made possible through financial support from the National Research Council of Canada under grant A-875 and from the Defence Research Board of Canada under grant 9931-10.

TABLE OF CONTENTS

INTRODUCTION

Much work is currently being conducted on self-organizing systems. The Conference on that subject held in Chicago, Illinois on May 22, 23 and 24, 1962, and attended by some 400 people whose backgrounds were divided among a number of scientific and engineering disciplines, evidences that fact. The simulation is the principal tool of the scientists in that respect. They look at existing specimens in order to build models which could be as perfect as the specimens themselves. They utilize the works of people in other fields, biologists, neurophysiologists, psychologists and others, in their search for improved systems. However, it must be admitted that if there are any simple rules for self-organizing, they have not been found yet.

The trend is to try to discover as many of the properties of the specimen as possible; direct introspection, mathematical and intuitive means are all equally good. The work described in the present report does not differ much from this line of action. The author has looked over the data from biologists and psychologists along with the works of his predecessors. Out of this information, has come the data necessary to render adaptive the up-to-then existing system of neurons or majority logic elements. Some data from other fields along with a short description of the existing equipment will be recalled before attempting to describe the present approach to a self-organizing system.

- CHAPTER 1 -

- THE HUMAN NERVOUS SYSTEM -

The Human Nervous System

To meet ever more complex and difficult problems, man is driving toward the perfection of electromechanical servants with a much higher order of intelligence. One of the most fascinating, promising approaches to the design of this new family of servants is through the application of the knowledge of biological systems to the solution of engineering problems. This is why the human nervous system, after all the most reliable computer in existence, will be briefly described. The types of learning will be investigated, along with a description of the learning process itself and of the main component of the system, that is the neuron.

Phenomena of retention and adaptation in organisms have been studied in a variety of experiments, differing greatly in their design. Memory experiments have been concerned with the retention and recall of experience, while learning experiments have been confined to the acquisition and modification of behaviour. Both types of investigation, however, deal with lasting modifications in the state of the organism and usually overlap each other.

1-1. Conditioning.[3]

First employed by Pavlov, this type of learning is characterized by the association of an existing response to a new stimulus, i.e. the generalization of responses from initial stimuli to

new stimuli. The original or unconditioned stimulus has an innate relationship to the response, while the substitute or conditioned stimulus has an acquired relationship.

This type of learning is best illustrated by the sequence shown below, in fig. 1-1. Initially, the response R can be elicited only by the unconditioned stimulus S_1. However, if we regularly

(a) (b) (c)

Figure 1-1

associate some other stimulus S_2, it might happen that the response R shifts from S_1 to S_2.

1-2. Trial-and-error.[3]

The original development of this type of learning process is due to Thorndike; it is concerned with the learning of a pattern of behaviour which is instrumental to the solution of a problem, or which satisfies a drive. The basic notion here is that living organisms have drives and that the response first made to a given drive in a given situation may not achieve the desired ends. Consequently, living organisms must have provision for response substitution, some means whereby a reaction

made originally, but inappropriately, to a given source of stimulation can be replaced by a more effective one.

Refering to fig. 1-2, at the left we note that some stimulus S produces a response R_1. But conditions change and R_1

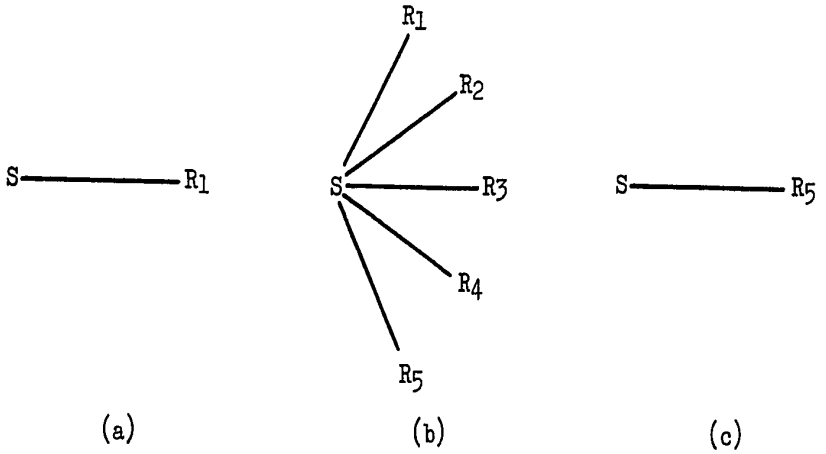

Figure 1-2

no longer responds to S. The organism then tries successively different responses R_1, R_2, R_3, R_4, R_5, the last of which produces the desired effect. On successive trials, R_5 gradually acquires more weight until it promptly and specifically follows whenever S occurs. This is trial-and-error learning.

1-3. Learning system.

In the biological nervous system, three classes of cells are generally distinguished: sensory, associative, and motor. It has been shown that simple perceptions are in fact complex: that they are additive, that they depend partly on motor activity, and that

their apparent simplicity is only the end result of a long learning process. We also have to remember that learning implies memory, that is, when we say that a person has learned we mean that his memory has somehow impressed the response.

Learning therefore could be defined as the process of acquiring the understanding of past events to be able to predict the future events. The human brain is a machine which gradually organizes itself to perform a given task as well as possible. This process of self-organization is the main characteristic of the nervous system and the one that we have to incorporate in our electromechanical "machines" if we want them to approach the perfection and the reliability of human beings.

The learning system can be described with the help of figure 1-3. Every cell shown has a characteristic threshold θ at which it responds. The sensory cells are the ones which are exposed to the physical stimulus. These sensory units are connected at random to the associative cells, only A and B in our case for simplicity, to which they send impulses. The connections from the associative cells to the response cells are also random. Once a response unit is initiated, it sends inhibitory pulses to other response cells and to the associative cells which do not participate in helping the proper response cell. The inhibitory pulses have a negative effect on the firing of cells.

Hebb's postulate[2] has also been accepted generally and is one of the basic tools to explain self-organization: "When

an axon of cell A is near enough to excite a cell B and repeatedly or persistently takes part in firing it, some growth or metabolic change takes place in one or both cells such that A's efficiency, as one of the cells firing B, is increased".

1-4. Description of the Neuron.

The neuron, basic nervous system building block, is ultimately responsible for the incredibly complex behaviour of the brain, including intelligence, learning and imagination. It may be briefly described - see fig. 1-4 - as consisting of a main cell body, from which runs an axon, a long fiber which may be regarded as a lossless transmission line. The axon terminates in a series of small dendritic branches, the ends of which lie on or near the cell bodies of other neurons. The point of near-contact between the dendritic endings and the succeeding cell body is termed the synapse or synaptic junction. The synapse is capable of transmitting an electrical impulse between one neuron and another.

Operation of the neuron is as fellows. If a sufficient number of nearly simultaneous impulses arrive at a set of nearby synaptic junctions, the potential of the cell body is raised above what is called the threshold potential, and the neuron fires. It is to be noted that the impulses can be either excitatory or inhibitory, the excitatory one decreasing the threshold and the inhi-

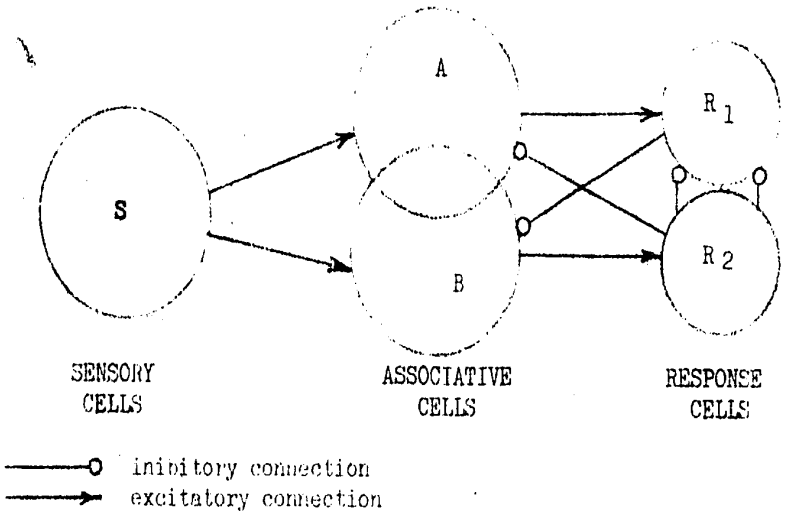

Figure 1-3

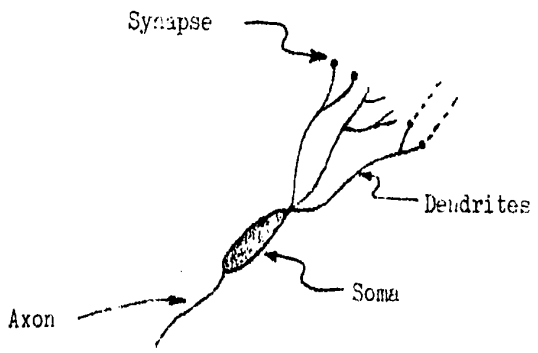

- Diagram of a Neuron -

Figure 1-4

bitory one increasing it. After firing, the threshold value rises instantaneously to a very high value and exponentially decays to the original value. This is referred to as refractoriness. The output of the neuron is a pulse of fixed amplitude and duration and, in that sense, the neuron can be called a transducer since the output is independent of the nature of the input signal, (it may be electrical or chemical for instance). The neuron also has the special property that the summation of inputs can take place within a certain time, typically of the order of a millisecond or so.

1-5. Random Net.

Each neuron, therefore, has logical properties similar to those of computer elements, that is the neurons in living organisms work on a threshold logic principle. Their behaviour could then be analyzed by propositional logic and a neuron could be represented by a threshold element. This element will be defined later in chapter 3, where a mathematical expression is found for the electronic neuron.

The vast number of neurons (around 10^{10}) in the human being constitutes a random net. In other words, the nervous system is a large set of similar and simply-acting elements whose attributes and interactive connections are randomly established. If neurons consequently could be properly simulated, interesting results could be obtained in the study of random networks. However, proper simulation means an adaptive neuron. The possibilities for self-organization of the equipment will investigated after a short review of the present form of the equipment.

- CHAPTER 2 -

- PRESENT FORM OF

UNIVERSITY OF OTTAWA

EQUIPMENT -

Present Form of University of Ottawa Equipment

The equipment presently available is centered around some electronic neurons and was used to perform experiments on adaptability and reliability. Before briefly describing these experiments, we will first have a look at the equipment itself and then at the electronic neurons.

2-1. Equipment[9]

As can be seen from fig. 2-1, all the necessary circuits are enclosed in a cabinet. The units are wired so that the drawers can be rolled out of the cabinet; the left side panel can also be opened for easy access to all parts. The equipment consists of a power supply (drawer D), neuron elements (drawer B), threshold adjustments (drawer A), pinboard for interconnection of the neurons (E), terminal board where the wires are brought out from the drawer (F), neon indicators (G), and switch board for selecting inputs (H). Pulse generators are used to provide the input pulses. Fig. 2-2 illustrates the wiring diagram of the cabinet, but only for one cell.

2-2. Neurons

The model used is a modification of the circuit developed by L.D. Harmon and R.M. Wolfe[6], The neuron possesses the main characteristics of the biological cell, as described earlier: all-or-none output, threshold, summation time, and refractory period.

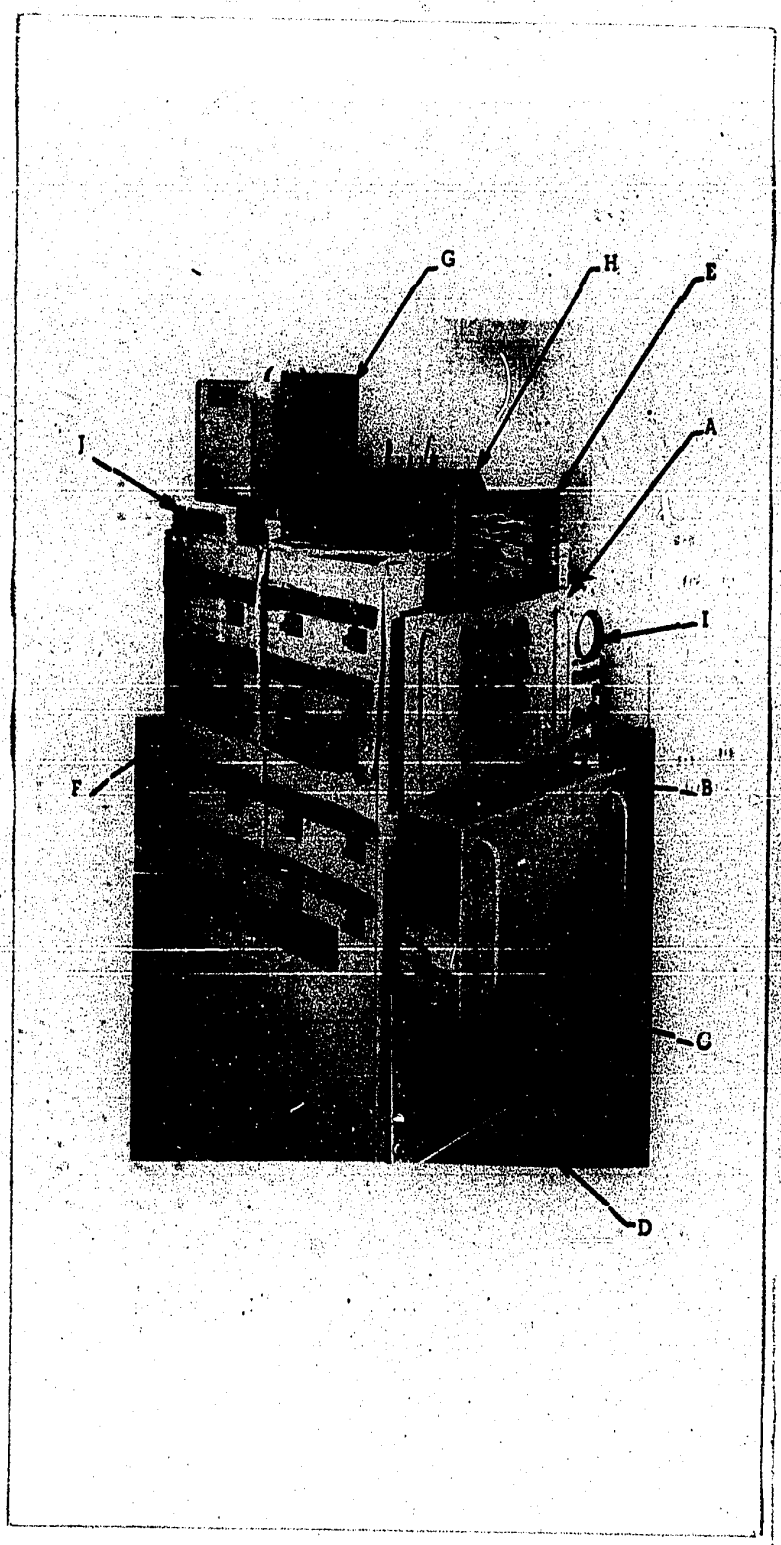

Figure 2-1

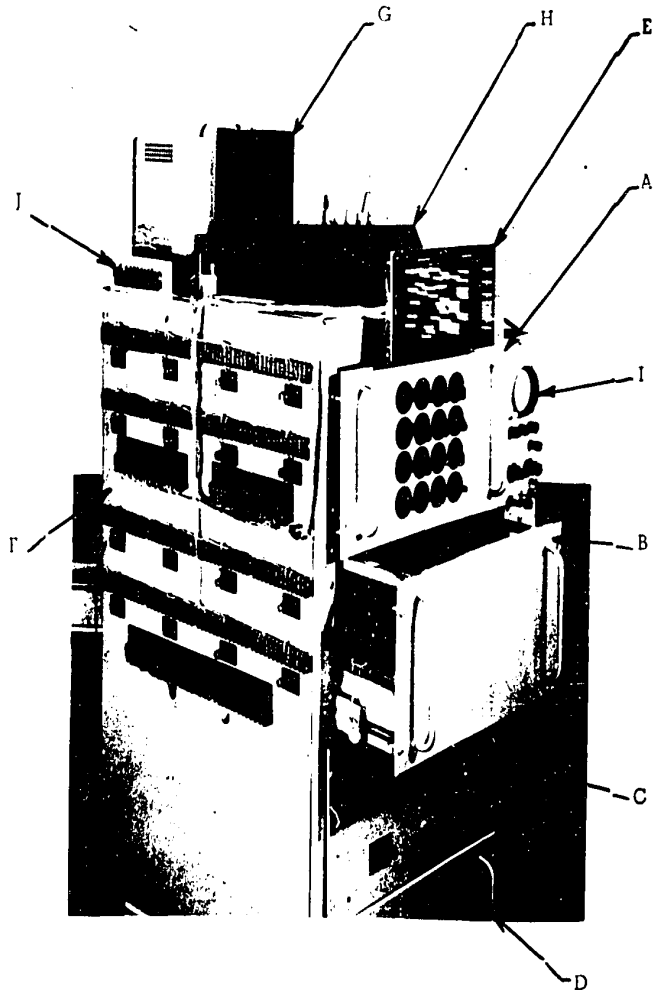

Figure 2-1

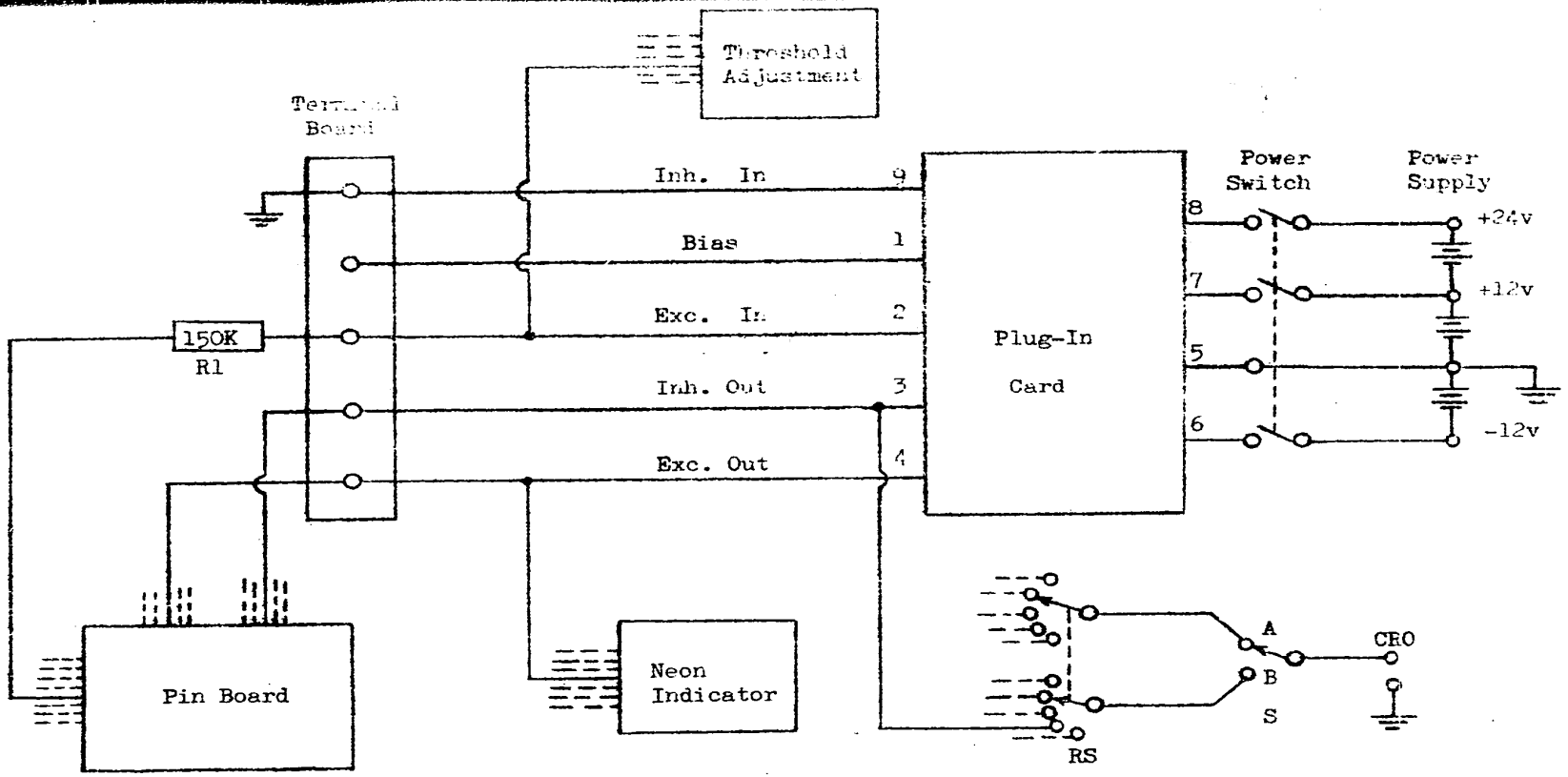

Wiring Diagram of Cabinet

Figure 2-2

A schematic diagram of the artificial neuron is given in fig. 2-3. Transistors T_1 and T_2 form the emitter-coupled monostable multivibrator, T_3 amplifies and inverts, while T_4 provide low impedance outputs. The emitters of T_1 and T_2 are at a potential θ_0 which represents the quiescent threshold of the circuit. Inputs are applied through resistances to the base of T_1 and are integrated by the action of capacitor C_1. When the summation of inputs is negative and larger than θ_0, transistor T_1 turns on and the firing action is initiated. The collector voltage of T_1 suddenly changes in a positive direction. Since a sudden change cannot take place across C_2, the positive change is coupled to the base of transistor T_2, turning it off. The time of discharge of C_2 determines the width of the pulse.

The absolute refractory period has two components. One is measured by the duration of the output pulse; the other is that interval immediately following, during which the largest input possible in the system cannot fire the circuit. The relative refractory period is a function of the recharging rate of C_2. Inhibition is accomplished by applying positive pulses on one or more of the inputs.

Description of experiments.[9]

The purpose of the different experiments on the above equipment was to study the problem of producing machines that are not fixed in their mode of operation from the beginning till the end by the will of their designer, but that are gradually modified by the inter-

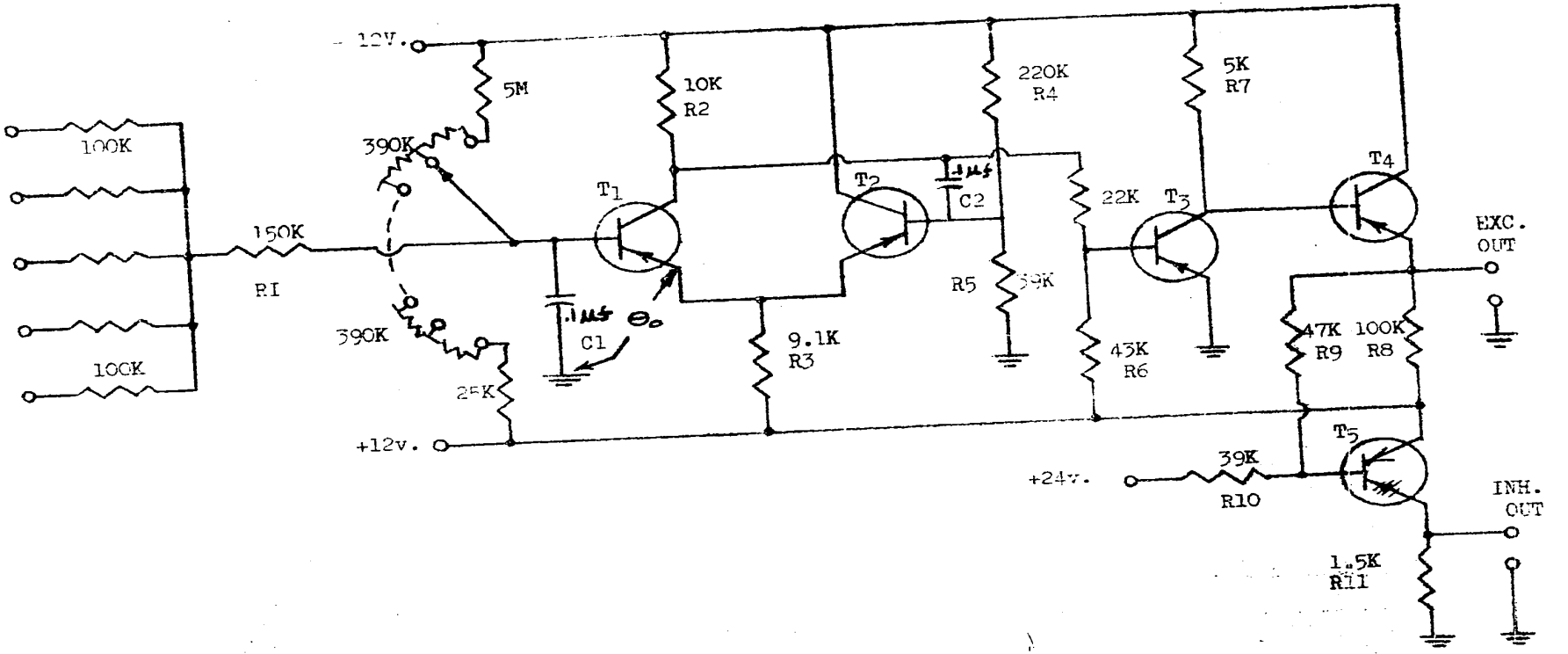

All Transistors
2N 224

Figure 2-3

vention of their operator, so that they gradually acquire more suitable characteristics.

Such a procedure is what is meant by learning, in the present case. The first set of experiments dealt with such learning while the second set was concerned with the reliability of the process. The second set on reliability, therefore, is dependent on the first one on adaptability and is consequent to it. Those experiments are very interesting and deserve, it is believed, a short description in the present text. It has to be remembered, though, as mentioned in the brief description of the equipment, that means are provided for the experimenter to externally help the machine to organize itself to perform a given task as well as possible.

The cells were first distributed in three groups, as in the human nervous system. The first group of cells simulated the sensory cells, the second one the associative cells and the last one the motor cells. As shown in fig. 2-4, the net was limited to two types of inputs and outputs for simplification purposes. It is obvious that the number of such inputs and outputs could be increased at the will of the experimenter.

The experiment on adaptability is divided in two parts: the learning period when the net is forced to yield the correct response and the testing period when the net is left to respond normally

to the excitation. This procedure, then, applies to both types of learning; the Pavlov's conditioning to force the correct output and Thorndike's trial-and-error to allow the net to adjust itself in the proper fashion. The system for self-organization of the cell, proposed later in this report, will make the above process automatic and will eliminate the need of external adjustments.

The reliability experiment studies the effect of neuron failure on the behaviour of the net. Neurons are made to fail one by one at random until the response of the net is changed. This tends to show that a single neuron, by itself, is not that important. The prime factor is the mass of cells which unite together to produce the action.

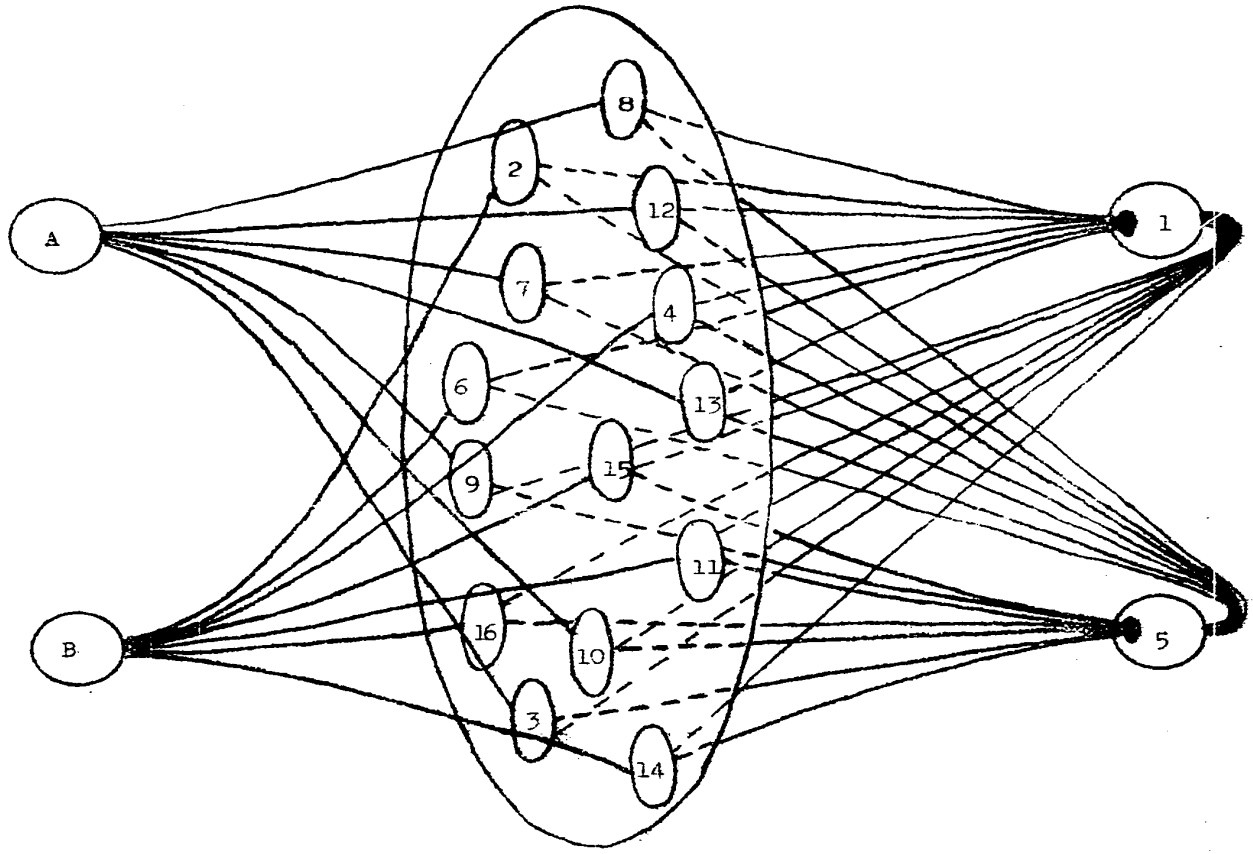
A
B
8
2
12
7
4
6
13
9
15
11
16
10
3
14
1
5
INPUT CELLS
ASSOCIATIVE CELLS
OUTPUT CELLS

Figure 2-4

- CHAPTER 3 -

- SELF-ORGANIZATION -

SELF-ORGANIZATION

After having studied the existing equipment, both theoretically and practically, we have reached the point where further improvement was desirable. We are particularly interested in the possibility of self-organization. What is meant by self-organization? Instead of a rather loose interpretation that the expression has had in the past, we will use the definition proposed by M.C. Yovits at the conference on "Self-Organizing Systems" in May 1962. "A self-organizing system is a system which changes its basic structure as a function of its experience and environment".

3-1. Methods of Self-Organization.

Many biological and social systems apparently exhibit behaviour which indicates existence of some changes or even optimization of the systems structure. Out of these examples has followed the description of a general system. As a consequence, the self-organizing systems are classed either as causal or goal-seeking.

A causal system changes its structure in response to the changes in the inputs, that is by means of changes in terms and relations. These changes occur due to the influence of the environment via modifications of a properly specified subset of terms, which could be the inputsfor instance.

A goal-seeking system, on the other hand, changes its structure in the attempt to achieve or pursue certain goals, i.e. by assigning a goal which the system is supposedly pursuing during its change. In many cases, objectives of a systems behaviour are apparent from the study of the actual systems behaviour or are postulated in the synthesis stage of the system.

Some central ideas now become apparent. First of all, for an effective self-organization, the system must have a decision making strategy. This decision making procedure is termed organizational since it presents an abstract model of organization. Then, to further improve self-organization of the overall system, the goal-seeking structure of organization might be changed; this is a self-organizing system.

3-2 Mathematical Representation of our Cell.

We have mentioned previously that our cells behave as logical elements. Fig. 3-1 represents a block diagram of one cell. It can be reduced to a mathematical expression as in fig. 3-2. It is termed a threshold element, a switching element in which each input x_i has two symmetrical units of some physical quantity which may be interpreted as $+1$ or 0, and for which there exists a set of real numbers $w_1, w_2, \ldots\ldots w_n$ called weights and T called threshold such that the output y is as follows:

$$y = 1, \quad \text{if} \quad \sum_{i=1}^{n} w_i x_i \geq T \qquad (3\text{-}1)$$

$$y = 0, \quad \text{if} \quad \sum_{i=1}^{n} w_i x_i < T \qquad (3\text{-}2)$$

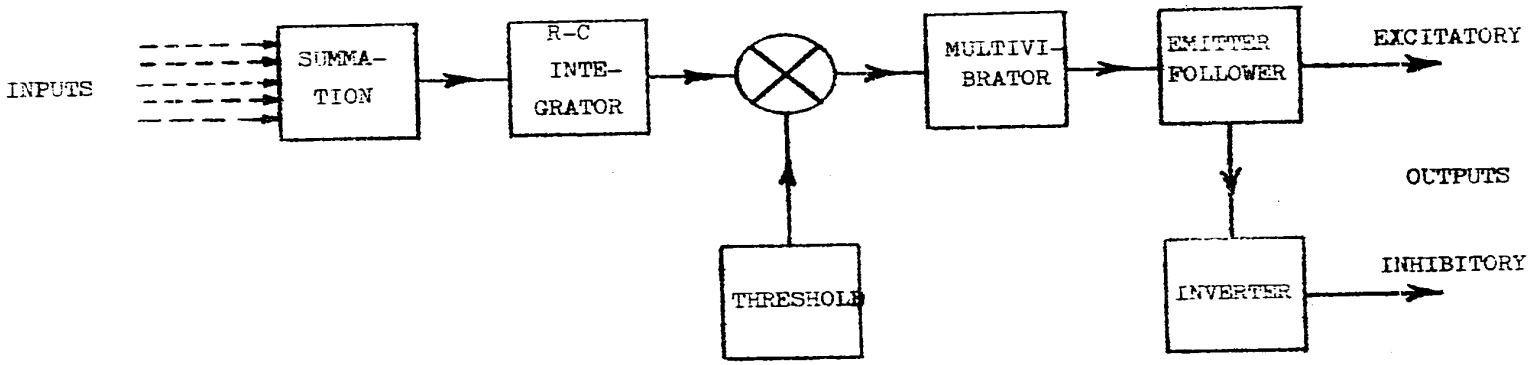

BLOCK DIAGRAM OF THE ELECTRONIC NEURON

Figure 3-1

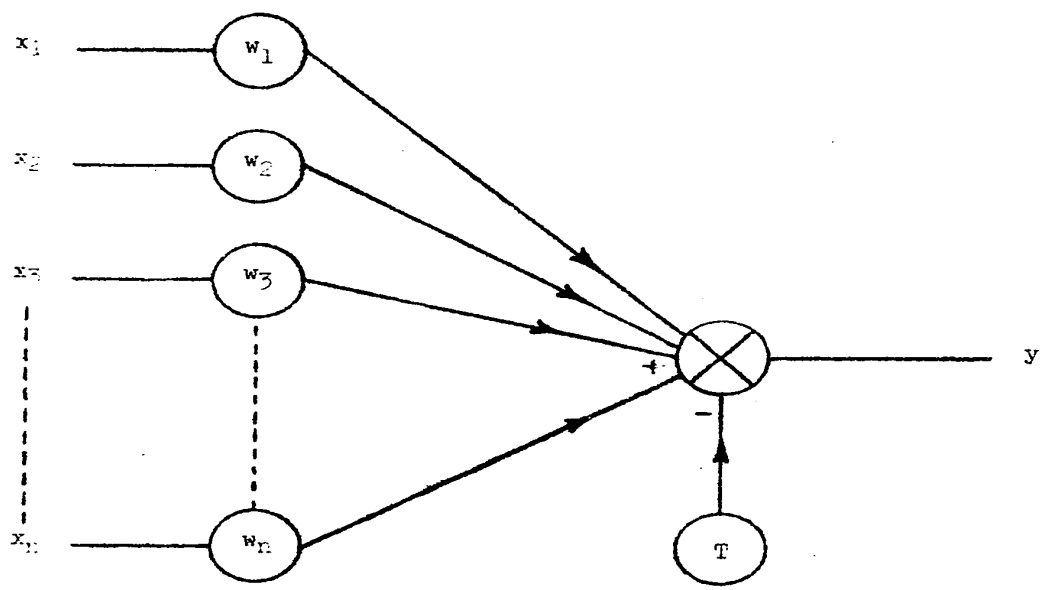

MATHEMATICAL REPRESENTATION

Figure 3-2

for any combination of values $x_1, x_2, \ldots\ldots, x_n$.

Consequently, the structure of our element is completely specified by its threshold T and the weights w_i;

$$y = f\ (w_1, w_2, \ldots\ldots, w_n; T) \qquad (3\text{-}3)$$

3-3. Possibilities for Self-Organization.

A quick glance at the equation (3-3) shows that there exist two possible solutions for self-adaptation problems; the first one is by means of the weights of the inputs and the second one through the threshold.

Both cases are illustrated in fig. 3-3. In the first case, the threshold T is fixed while the weight w_i is variable; w_i is a measure of the importance of x_i in the system. The actual output is then compared to the desired one and adjustments follow. Correcting factors will be slowly added to w_i in the right direction, i.e. in the direction that will make the error between the actual and the desired outputs converge toward zero.

In the second case, the weights w_i's of the inputs x_i's are all fixed; the threshold is now the variable. Again, the result of the comparison between the desired and the actual outputs will affect T in such a way as to make this error tend to zero.

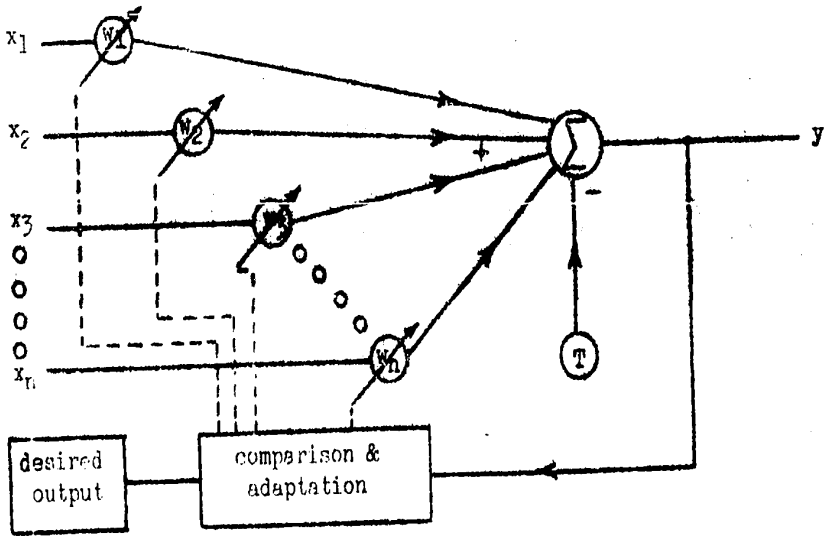

VARIATION OF INPUT WEIGHTS

Figure 3-3a

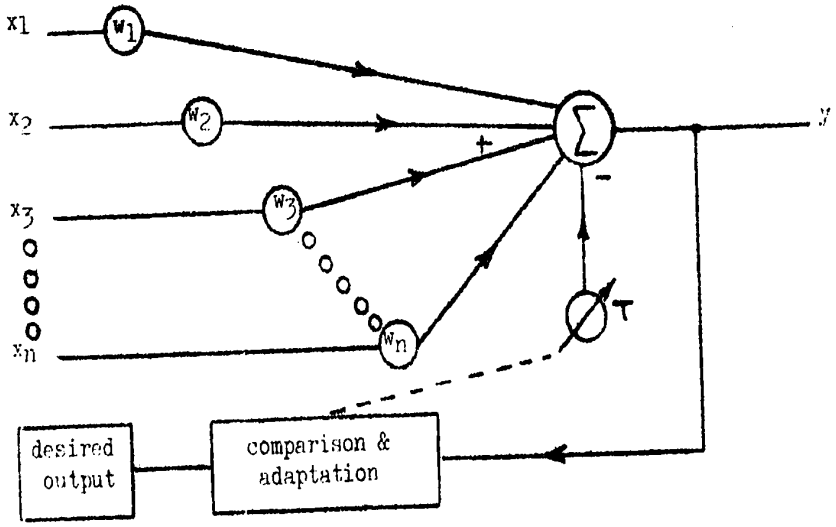

VARIATION OF THRESHOLD

Figure 3-3b

Obviously, both cases could be applied practically to our present equipment. However, we will restrict ourselves to the second type for the moment, that is the type where the threshold varies and the inputs are fixed. In the next chapter, we will outline the basis of our proposed system. Before doing so, we would like to review briefly some existing self-organizing system hardware.

3-4. Existing Systems.

3-4a. Perceptron.[10,19,20]

Rosenblatt first reported on the Perceptron in 1958. It represented a major attempt to place the complete learning sequence of an artificial nerve-net on a rigorous mathematical basis. Perceptrons in general may be described as a class of minimally constrained nerve nets consisting of logically simplified neural elements. Rosenblatt succeeded in proving that learning of an input-output relationship will indeed occur in a linear-summation network under very general conditions of repeated presentation of input and desired output patterns. It is necessary that synaptic strengths or weighting elements follow certain rules of growth, and that a solution exists for the set of values of the weighting elements required to realize the given output function.

A simplified form of the Perceptron model is

illustrated in fig. 3-4. It is assumed that sensory inputs are mapped by means of random connections with fixed synaptic strengths upon a series of neurons termed A-units. The responses of the A-units are then mapped through variable connections to a set of response-units (R-units) which determine the outputs (only one shown).

During the learning process, the values stored in the W-units are changed whenever the state of the output R_j does not correspond to some arbitrary desired response D_j for the given input pattern. This is error correcting "forced" learning. Whenever it is necessary to correct a response, the strengths of all synaptic junctions (W-units) connected to that output change simultaneously according to some simple rule.

Verification of network learning has been obtained both by means of digital computer simulations and by experiments on a hardware model of the Perceptron system. The latter possesses 400 inputs in a 20-by-20 array, approximately 400 A-units, and 8 R-units. It makes use of magnetic integrators as storage for experience data. The value of magnetic flux stored in the integrator represents the present state of the machine and must be changed to obtain new states. This change is brought about by logical rules whose selection is based on experience and theory.

3-4b. Memistor Adaline.[13,16]

Widrow considers the learning process from the

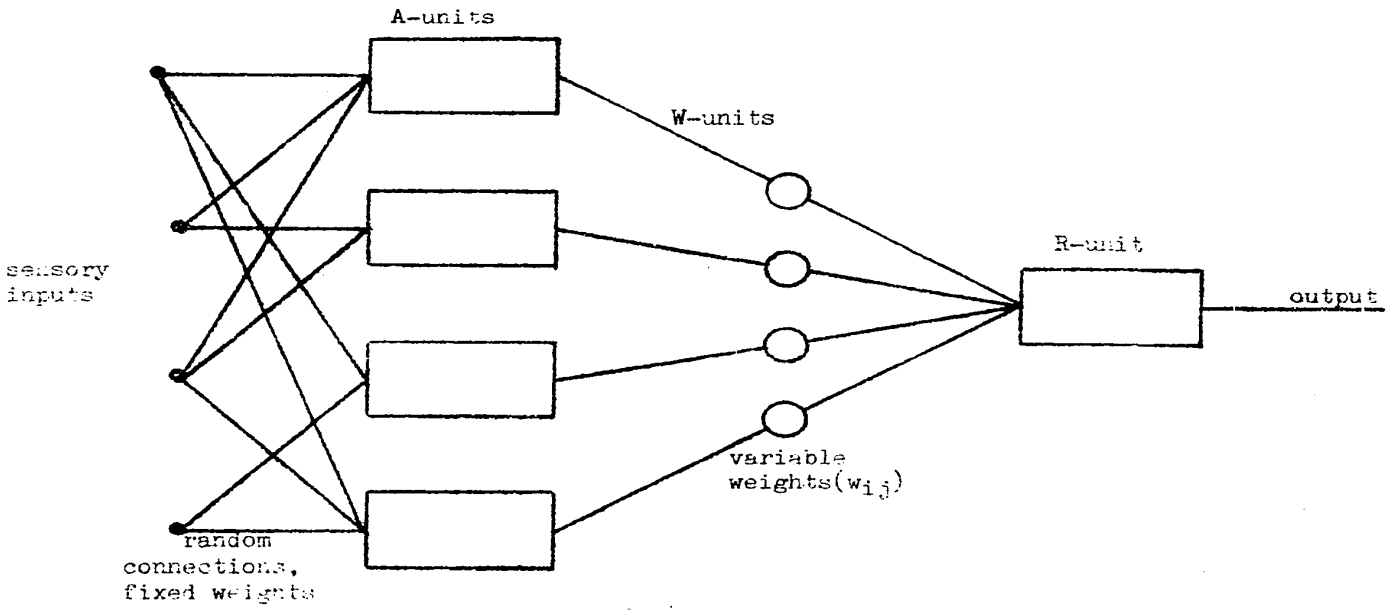

- PERCEPTRON MODEL -

Figure 4-1

point of view of minimizing the mean-square-error between the obtained and desired outputs over the set of patterns. To perform experiments, he has designed an adaptive logical element called the ADALINE (ADAptive LInear NEuron) whose block diagram is shown in fig. 3-5. It is seen that the adaptation is obtained through variations of weights and threshold.

In large networks however, it became imperative that the adaptive processes be fully automated. For this purpose, a new electrochemical element, a resistor with memory, called MEMISTOR, was designed. It provides a single variable gain element; each adaline therefore employs a number of memistors equal to the number of input lines, plus one for the threshold.

A memistor consists of a conductive substrate with insulated connecting leads, and a metallic anode, all in an electrolytic plating bath. The conductance of the element is reversibly controlled by electroplating. It is a three terminal element; the conductance between two of the terminals is controlled by the time integral of the current in the third terminal. Adaptation is accomplished nondestructively by passing alternating currents through the array of memistor cells.

A circuit for a memistor adaline is shown in fig. 3-6. The input signals are applied by means of switches and the

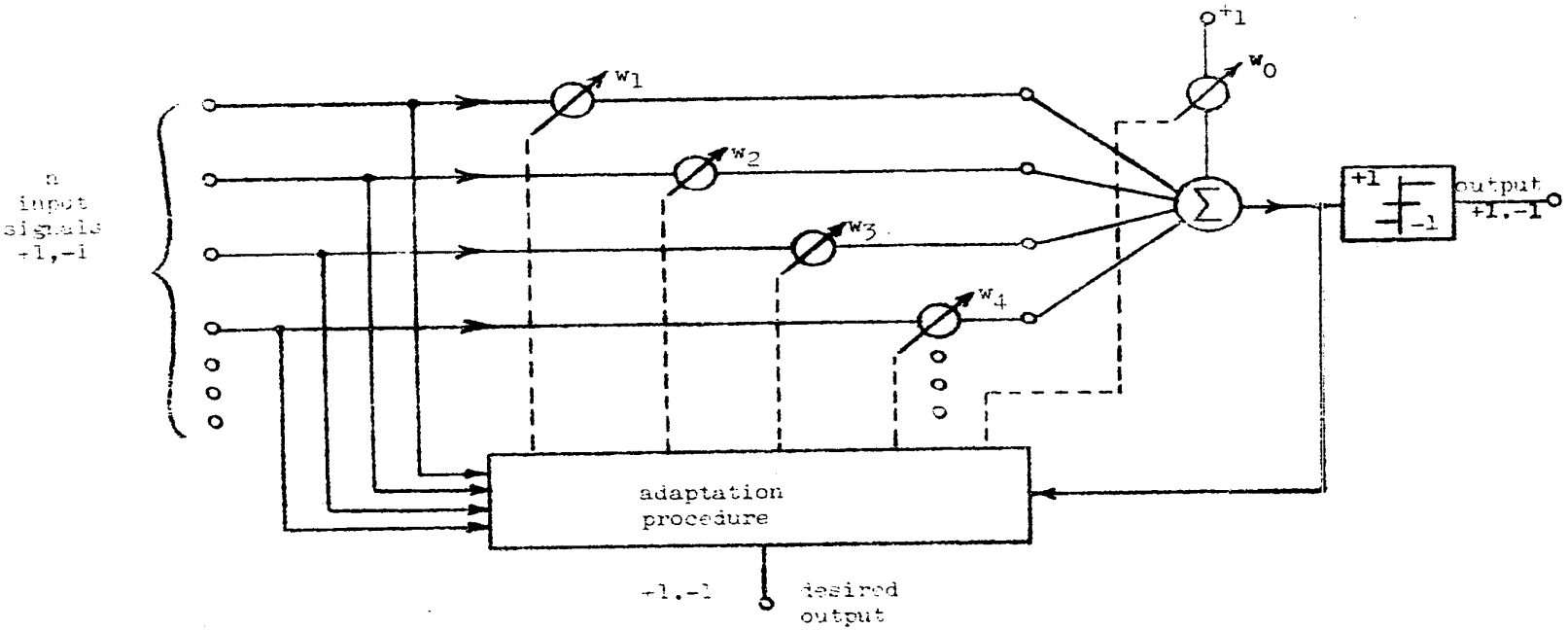

- BLOCK DIAGRAM OF THE ADALINE -

Figure 7-5

over-all direction and extent of adaptation are controlled manually. The direction in which each memistor should be adapted is determined by the algebraic product of the error signal multiplied by the particular input signal. This product acts directly on the input pattern in such a manner as to minimize the error between the actual and desired outputs.

The effect of positive and negative gain values is obtained by balancing the memistor against a fixed resistor in a bridge arrangement. The sensing of the gain is done by applying an a-c voltage to the memistor, and another a-c voltage with a 180-degree phase difference to the fixed resistor. The currents are proportional to the conductance and are summed. An individual gain is zero when the memistor conductance equals that of its reference, and an ideal value of reference conductance is the average of the conductance extremes of the memistor.

3-4c. G.E. Adaptive Neuron.[24]

The work undertaken by General Electric has been confined to a single cell with the assumption that the behaviour of the neuron would not be affected when incorporated in a network. A brief description of the cell will be followed by outlining the self-organizing feature.

The block diagram of the neuron is shown in fig.

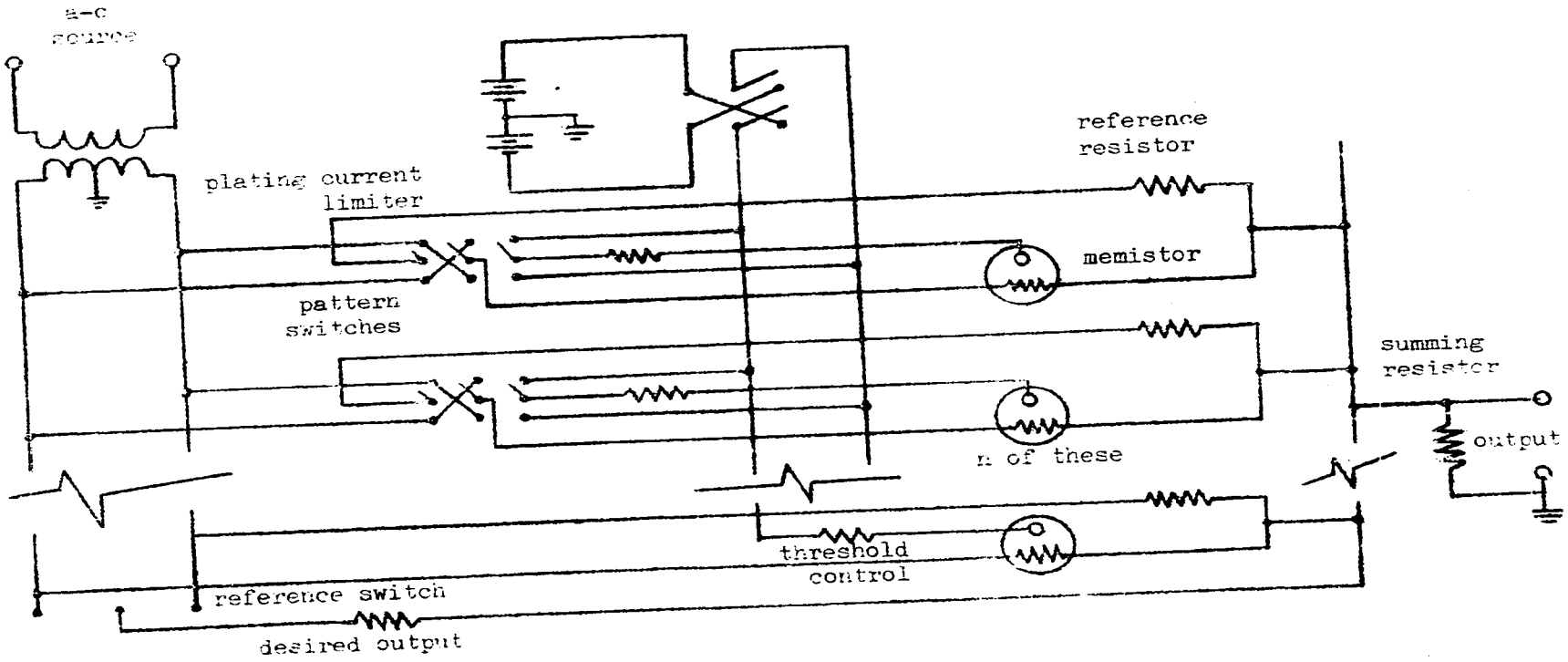

MEMISTOR ADALINE

Figure 3-6

3-7. The weighted positive inputs and the constant negative inputs are summed algebraically in a resistor network; when the sum exceeds the threshold level the cell fires. The output is a standard pulse. This pulse is fed back to all of the input coindence gates. The coindence of this pulse and an exciting input pulse causes the gain level in the active channel to be increased by a fixed amount. Consequently, the gain level is increased in each input channel which has contributed to the firing of the cell.

The self-adapting features are primarily associated with the weighted inputs; the transfluxor (fig. 3-8), a device utilizing flux integration, performs the major portion of the memory function. The exciting windings are used to indicate the state of the transfluxor; one pulse signal on winding A switches the output leg (readout winding) while another pulse signal on winding B resets it. This exchange of flux between the output legs is directly proportional to the flux stored in the main body of the transfluxor; it also does not alter in any way the level of the transfluxor.

The signal from the coindence circuit associated with the input multiplier is fed to the transfluxor unblocking winding. It causes the flux in the output leg to increase which in turn increases the output signal. The stored gain level decreases by applying pulses to the "forget" winding. Those pulses can be adjusted externally to achieve any desired decaying rate. The gain level decreases by a samll amount each time a forget signal - high current short duration pulse -

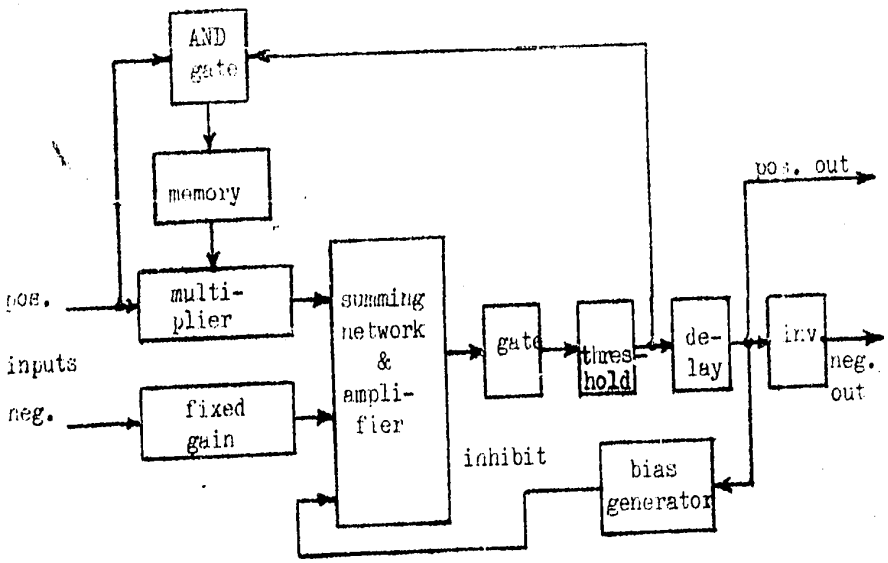

BLOCK DIAGRAM OF NEURON

Figure 3-7

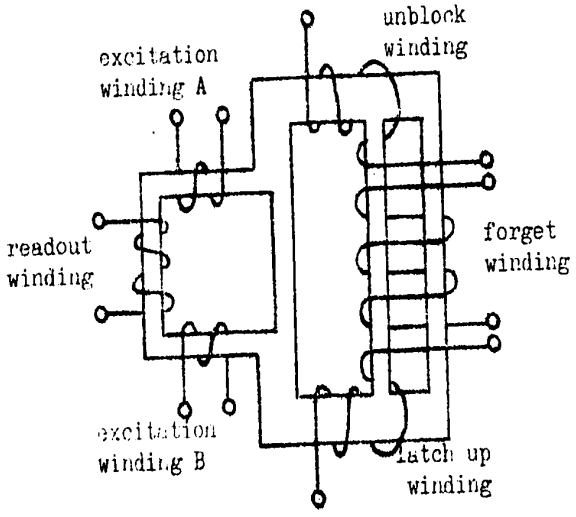

TRANSFLUXOR

Figure 3-8

is applied. The latch up winding is used to maintain the transfluxor in the maximum gain position, when it reaches it, regardless of the forget signal.

It is seen that the above cell closely resembles the human nervous cell. The firing of the neuron once makes it easier for the cell to fire a second time if properly stimulated. However, this feature does not last forever in the human brain and this is simulated by the decaying rate of the gain level. On the other hand, only the working cells have their thresholds raised; the non-firing cells remain in their original state.

3-4d. Melpar - Artron.[14]

The ARTRON (ARTificial neuRON) in the present case is rather a logical element where the output c is some logical function of the inputs a and b.

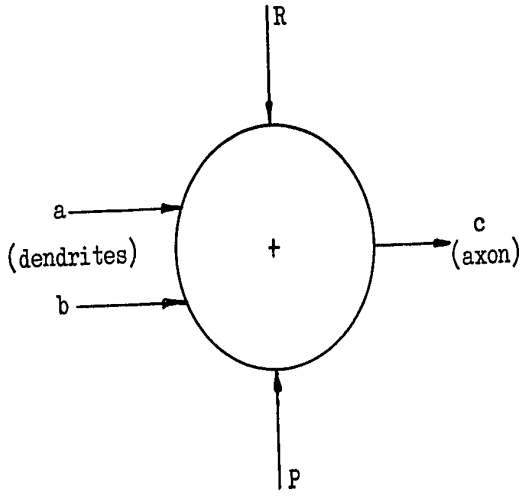

Figure 3-9

Teaching the artron is essentially a process of changing the probability of existence of any state through the channels R (reward) and P (punish). The utility of these elements appear only when they are interconnected into a network. The system is based on the assumptions that "a reasonably large and more or less randomly connected network has, as one subset of its possible states, particular states which produce the desired functional output from the given inputs and that the system is given sufficient time for the goal directing reward and punishment mechanisms to effect the organization".

Networks of artrons are capable of learning to perform Boolean function operations and of implementing decision processes; they are also used to simulate elementary human behaviour patterns. Up to now, three neurological subsystems (color and tone recognition, hand-eye coordination and the maze runner) have been simulated. The most interesting experiment is undoubtedly the last one, where a vehicle based on artrons was built with most of the known functions of the rat. This vehicle is then taught to reach a given point by using the shortest path.

The variation of the probability is performed through statistical switches. As learning progresses, the statistics are biased toward a probability of 1 or 0. The switch uses magnetic storage. The transfluxor provides this function as well as a non-destructive memory.

- CHAPTER 4 -

- PROPOSED DEVELOPMENT -

PROPOSED DEVELOPMENT

From the previous discussion on self-organization, the following characteristics need to be inserted when developing such a system:

1. a change in the firing conditions of the cell (which was pointed out in eq. 3-3);
2. a memory (by this is meant a system which could recall the past experience in dealing with the present problems);
3. a non-destructive read-out, (so that the state of the device could be indicated at any time without disturbing that state in any way).

4-1. Possible Developments.

In the light of the above characteristics, an attempt will be made to review the more salient features of possible memory schemes. This brief analysis should allow us to make the optimum choice in the present case.

4-1a. Charged Capacitors.

The engineer always associates the concept of memory with a capacitor. The fact that capacitors accumulate and retain charges for a certain time can certainly be interpreted as a sign of memory. An indication of the voltage across the capacitor is a read-out,

but not necessarily non-destructive, as it will be seen.

It is reasonable to consider a 1000 ufd as an upper bound of commercially available capacitors. In order for the memory to last 10 hours, i.e. the time constant to be 10 hours, a simple calculation shows that the leakage resistance should be 36 megohms.

$$\tau = rc$$

$$r = \frac{\tau}{c} = \frac{10 \times 3600}{1000 \times 10^{-6}}$$

$$= 36 \text{ megohms}$$

Although this figure is reasonable, a voltage sensing device of higher input impedance is required. Similarly, the network necessary to add charges must be such as not to load this figure down.

It is normally desired also, in such a system, to have equal increments through the adaptive procedure. This is particularly difficult to achieve with capacitors since it means adding just enough charge to a partially charged capacitor in order to increase its voltage by a constant amount; since the time spent by the capacitor in anyone state is never the same, the number of charges lost in that period is not constant and is unknown. The large time constant, on top, brings the disadvantage of making this change of state a long affair.

4-1b. Electromechanical Devices.

The main characteristic of such a device consists, of course, of its stability, since proper contacts are achieved through mechanical displacements. Such a system is rather easy to design but the size and costs become extremely large. Although the size is not a factor in the present case, it could become one, should it be decided to increase the number of units.

The operating time is obviously very slow and cannot possibly approach rates of biological systems. This drawback is sufficient to reject such a prospect.

4-1c. Flux Integration.[12]

The idea of flux integration comes from the core memories of digital computers. Without going to a rigorous treatment, a quantitative understanding may be gained by consideration of the dynamic hysteresis loop of the core material.

Consider a toroid as shown below.

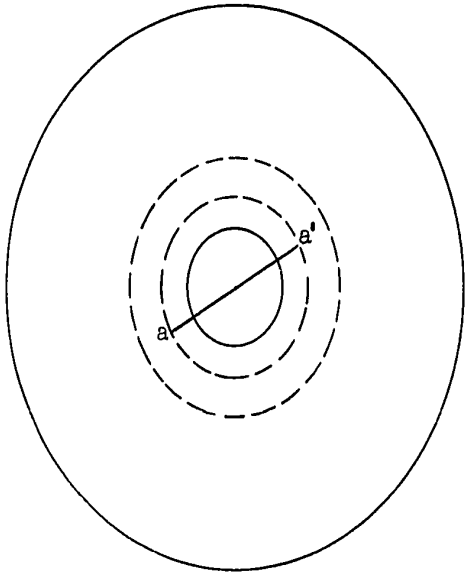

Suppose the core is in a partially saturated condition, up to aa'. If now a magnetomotive force is set up in the direction of the previous magnetization, the domains most affected are the ones in the region immediately surrounding the boundary of magnetization, since the m.m.f. affects primarily the domains for which the path is shortest.

The linearity of the flux increase with respect to the number of input pulses can be very good by selecting the proper material for the toroid. A non-destructive read-out can be obtained by using the principle of the transfluxor.

The speed of the response is very good and it is obvious that either positive or negative increments can be obtained.

4-1d. Variable Resistors.

By variable resistors, are meant simple devices like thermistors. Other sophisticated elements, like mistors which are based on a variation of flux density, fall in other categories and are not implied in this section.

The currents that flow through a thermistor raise its temperature through ohmic dissipation, and the temperature characteristics of the device are such that its conductance is thereby

increased. If the thermistor can be maintained in this non-equilibrium state, it will be able to pass larger current for succeeding stimuli.

The nature of this weighting device obviates the need for any auxiliary circuit. Unfortunately reinforcement is strictly one way. Another drawback is the short memory of thermistors: it is only of the order of three to four minutes and it is doubtful That the simplicity and low cost of the device can overcome its disadvantages.

4-2 Selection and Approach.[27]

From the brief review outlined above, it appears that the flux integration shows the greatest future and complies the best with the necessary conditions. Consequently, this method was selected for an attempt to make the existing cells self-adaptive.

Our plan is to utilize the properties of the Hall element with the ones of a square-loop ferromagnetic materiel. The voltage supplied by the Hall element will directly modify the threshold of the neuron and will therefore bring the required changes in the firing conditions; this voltage will also be an indication of both the present state of the cell and of its past history. On the other hand, the flux stored in the ferromagnetic material will provide the memory.
Let us, for the moment, look at the theory and properties of both the Hall element and the square-loop ferromagnetic material, in

order to find out the best way to tie them together.

4-3. Hall Effect.[25,32]

The Hall effect, although it was discovered in 1879, has been explained rather thoroughly only in the last few years, when some engineering applications were developed. The phenomenon which essentially characterizes the Hall effect will first be recalled.

Consider a semi-conductor (see fig. 4-2) placed in a magnetic field perpendicular to the direction of current flow; a voltage will then be developed across the specimen in the direction perpendicular to both the current and the magnetic field. The voltage is called the Hall voltage. It is developed because the moving charges making up the current are forced to one side by the magnetic field. The charges accumulate on the side of the specimen until the electric field associated with the accumulated charges is large enough to cancel the force exerted by the magnetic field.

Let the specimen be a thin slab where the lenght "l" is much larger than the thickness "t"; then the Hall voltage V_h can be expressed as:

$$V_h = \frac{R_h}{t} (\bar{I} \times \bar{B}) \qquad (4\text{-}1)$$

where R_h is the Hall constant.

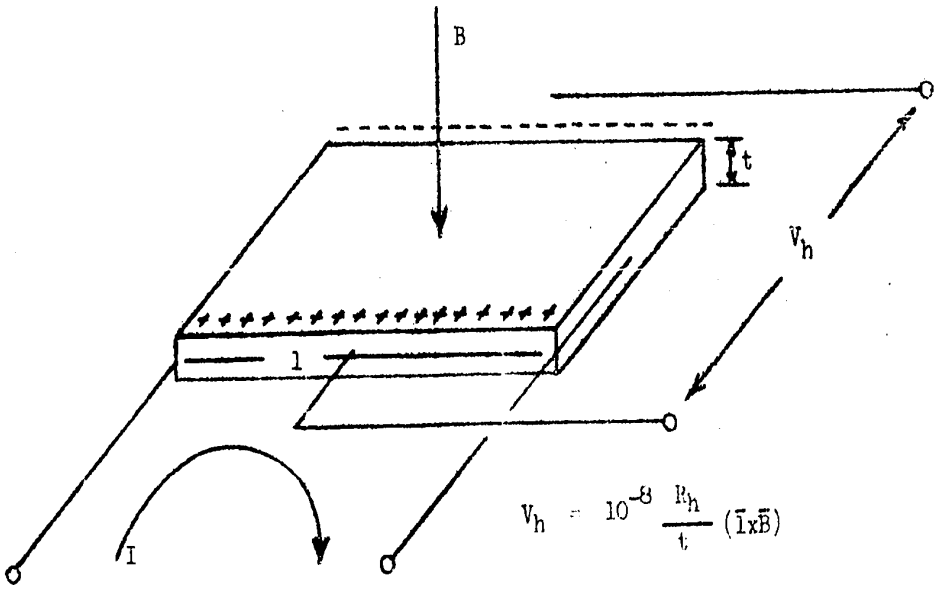

HALL EFFECT

Figure 4-2

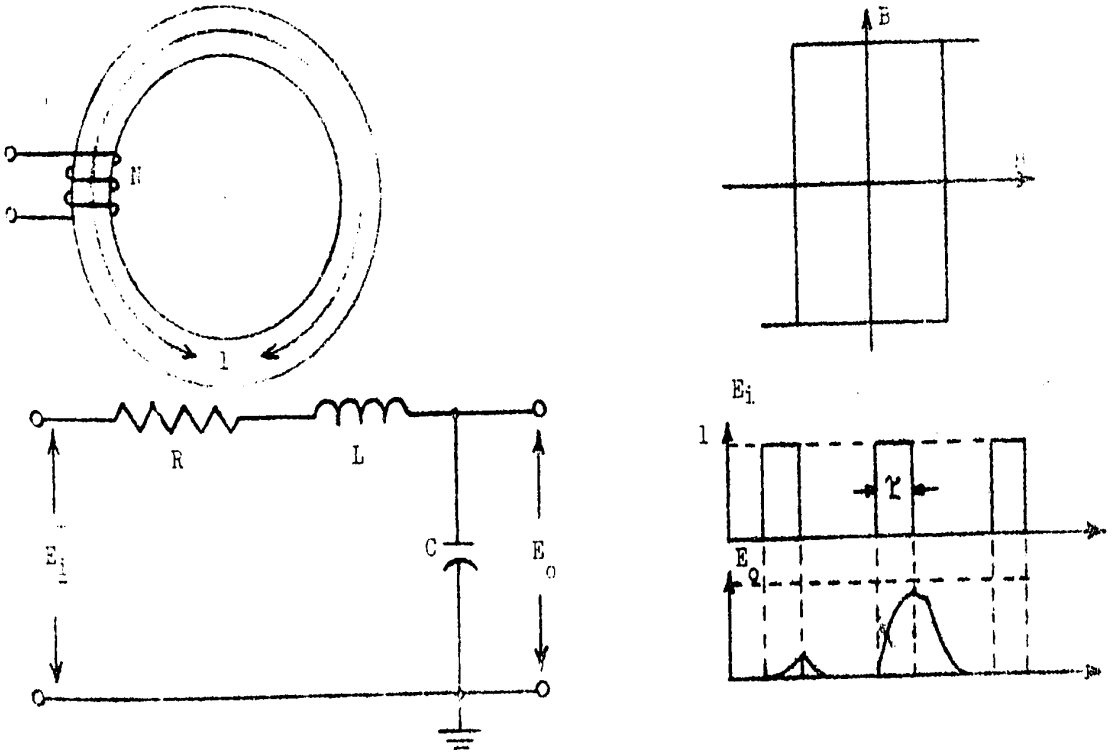

BINARY OPERATION

Figure 4-3

$$\text{or:} \quad V_h = \frac{R_h}{t} \left| I \right| \left| B \right| \sin\theta \qquad (4\text{-}2)$$

It appears, from what was said above, that the angle θ between the magnetic field B and the current I is 90^0.

Therefore: $\sin\theta = \sin 90^0 = 1$

and equation (4-2) becomes:

$$V_h = \frac{R_h}{t} I \cdot B \qquad (4\text{-}3)$$

Expressing t in cms instead of meters and B in gauss instead of webers we finally obtain:

$$V_h = \frac{R_h}{t} 10^{-8} I \cdot B \qquad (4\text{-}4)$$

where V_h is in volts

R_h is in cm^3/coulomb

t is in cm

I is in ampere

B is in gauss

It is also known that the Hall coefficient is expressed by the following relation:

$$R_h = \frac{1}{ne} \qquad (4\text{-}5)$$

where e is the carrier charge,

n is the density of free carriers.

It is to be noted that the absolute value of e is the absolute value of

the electron charge, whether the carriers are holes or electrons; the difference is only in the sign.

4-4. Square-loop Material[28,29,30]

Our interest in such types of materials lies in the fact that it is possible to have them in different states. Let us first consider a simple circuit for a binary state (bi-stable) operation. Then we will investigate how this could be increased to a multistate affair.

4-4a Bi-stable Operation

Consider the circuit shown in fig. 4-3. It consists simply of a capacitor in series with a coil wound on a toroidal core of square-loop magnetic material. The input E_i consists of unidirectional voltage pulses whose volt-time areas are all equal. The response of the circuit is also illustrated; the first pulse switches the core L from negative remanence to the positive one; the voltage across the capacitor during this time is small. At the end of the pulse, the capacitor discharges through L and R, but the magnitude of this discharge current is such that it does not exceed the coercive current; consequently, there is no resetting of the core flux. During the time interval of the next input signal, the output E_o is a relatively large voltage, equal to the input less the voltage across R. At the end of this second

pulse, the capacitor C is charged to a value nearly equal to the input voltage, since the core is already saturated in that direction. At the termination of the pulse then, C discharges through L and R. This resets the core to negative saturation, in preparation for another cycle.

Such a circuit, therefore, could easily be applied as a counter to the base of two. It could equally well be considered as an element with two different states, 1 and 0, for dealing with symbolic logic.

4-46. Multi-state Operation

Until recently, most circuits available for digital applications were binary in operation. From research and development, however, has come the multi-pulse magnetic counter, where the core of square hysteresis loop material is driven in a number of discrete steps from one saturated state to the opposite one. In other words, increments of magnetism are added to the loop until the core is saturated.

Effectively, to change a core from one remanent state to another, an applied pulse must have a voltage-time equal to the maximum flux of the core times the number of turns on the winding. This follows directly from Faraday's law; the law states that the voltage

across a winding is equal to the time rate of change of flux linkage:

$$E = N \frac{d\phi}{dt} \tag{4-6}$$

On integrating this formula with respect to time, the total area of the pulse is equal to the number of turns times the maximum flux variation in the core, for a pulse producing full switching:

$$\int_{-\phi_r}^{+\phi_r} d\phi = \frac{1}{N} \int_0^{\tau} E dt \tag{4-7}$$

$$\therefore \quad 2\,\phi_r = \frac{1}{N} E.\,\tau \tag{4-8}$$

Assume an ideal core. Further, suppose that one applies pulses which are much smaller than the one which is just large enough to switch the core. In this ideal case, it would require "n" such pulses applied to a winding on the core to switch it if each pulse is $\frac{1}{n}$ of the minimum amplitude and duration.

However, no core is ideal; the slope of flux over magnetic field is always finite. The curve of fig. 4-4 is a typical one. It is seen that, when a core is switched only part way, there is a fallback of flux $\Delta\phi'$ which occurs as the drive pulse is removed. It is wrong, consequently, to divide equation (4-8) by "n" if "n" states are desired.

Consider, to take a practical case, that this fallback averages about five percent of the total core flux; then to

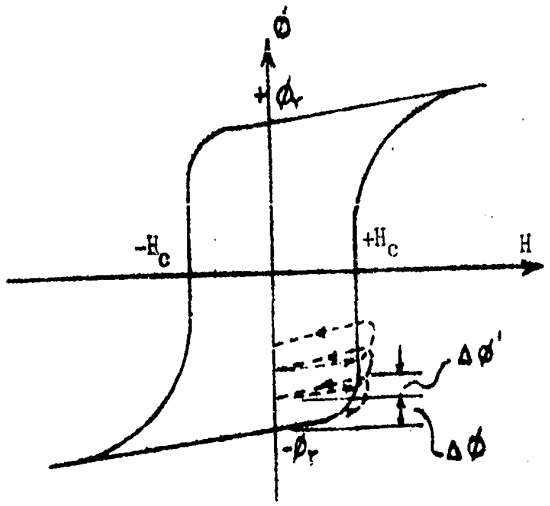

MULTI-STATE OPERATION

Figure 4-4

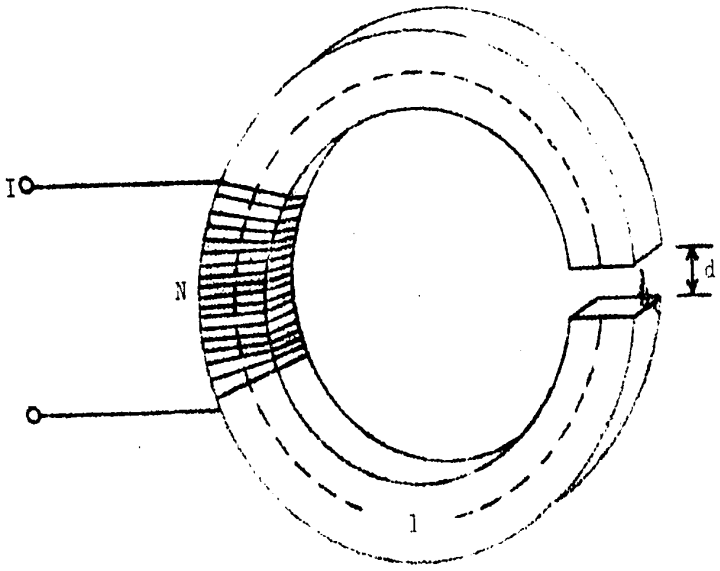

AIR GAP

Figure 4-5

switch the core in "n" steps, one loses the fallback after each of the first (n-1) pulses. The total area under all "n" pulses must thus be [100 + (n-1)5] per cent of the area under a single pulse which could itself completely switch the core.

4-5. Air Gap.[34,36]

Our proposal is to make an assembly out of a Hall element and a square-loop material. Since, as it was mentioned earlier, the flux must be perpendicular to the direction of both current and voltage, this means effectively cutting the core, in other words making appreciable changes to the B-H curve. Of course, it is desired to render this effect negligible on the core. Before trying to cure the defects, let us see what they are.

Consider a toroid with an air gap of width d, (see fig. 4-5). Let also the length of the magnetic path around the material be l. Assume, for simplicity, that the parallel-faced air gap is perpendicular to the flux direction and that all the flux lines follow the iron and cross the air gap without refraction.

Consequently, the flux densities in the iron and in the air are equal:

$$B = B_i = B_a = \frac{\phi}{A} \qquad (4\text{-}9)$$

where B_i = flux density in the iron,

B_a = flux density in air,

ϕ = flux,

A = cross-sectional area of the toroid.

The closed-path m.m.f. is then given by:

$$F = NI = H_i l + H_a d \tag{4-10}$$

or:
$$F = B\left[\frac{l}{\mu_i} + \frac{d}{\mu_o}\right] \tag{4-11}$$

where μ_i is the permeability of the iron,

μ_o is the permeability of air.

By permeability, is meant the static permeability, i.e.:

$$\mu = \frac{B}{H} \tag{4-12}$$

(4-10) can also be rewritten in the following manner:

$$F = l\left[H_i + H_a \frac{d}{l}\right]$$

$$= H_r \cdot l$$

where H_r is the equivalent magnetic field for the combination of iron and air gap in series.

Some interesting conclusions can be drawn from the above equations. First, the effective permeability of the air gap is

the permeability of air multiplied by a factor 1/d. Also, since the flux density is identical everywhere, the resultant magnetic field is the sum of the magnetic field in the material plus a factor d/l times the magnetic field in the air.

The resultant B-H curve, therefore, can be easily computed in a graphical fashion. As illustrated by fig. 4-6, the B-H curve for the material is first drawn in and then the one for the air gap. The grapnical summation, horizontally, of these two curves yield the resultant curve. It is seen that the angle d is determined by the following relation:

$$\tan \alpha = \frac{B}{H} \qquad (4\text{-}14)$$

This last relation, obviously, holds only in the c.g.s. system where the permeability of air is one gauss/oersted.

4-6. Proposed System.

Up to now, we have looked at all the elements, individually, which shall make up our self-organizing scheme. We know now that the principal component is the neuron, that we will attempt to make it self-adaptive through its threshold variation, that this should come about through the use of a square-loop material which is cut in order to insert a Hall element.

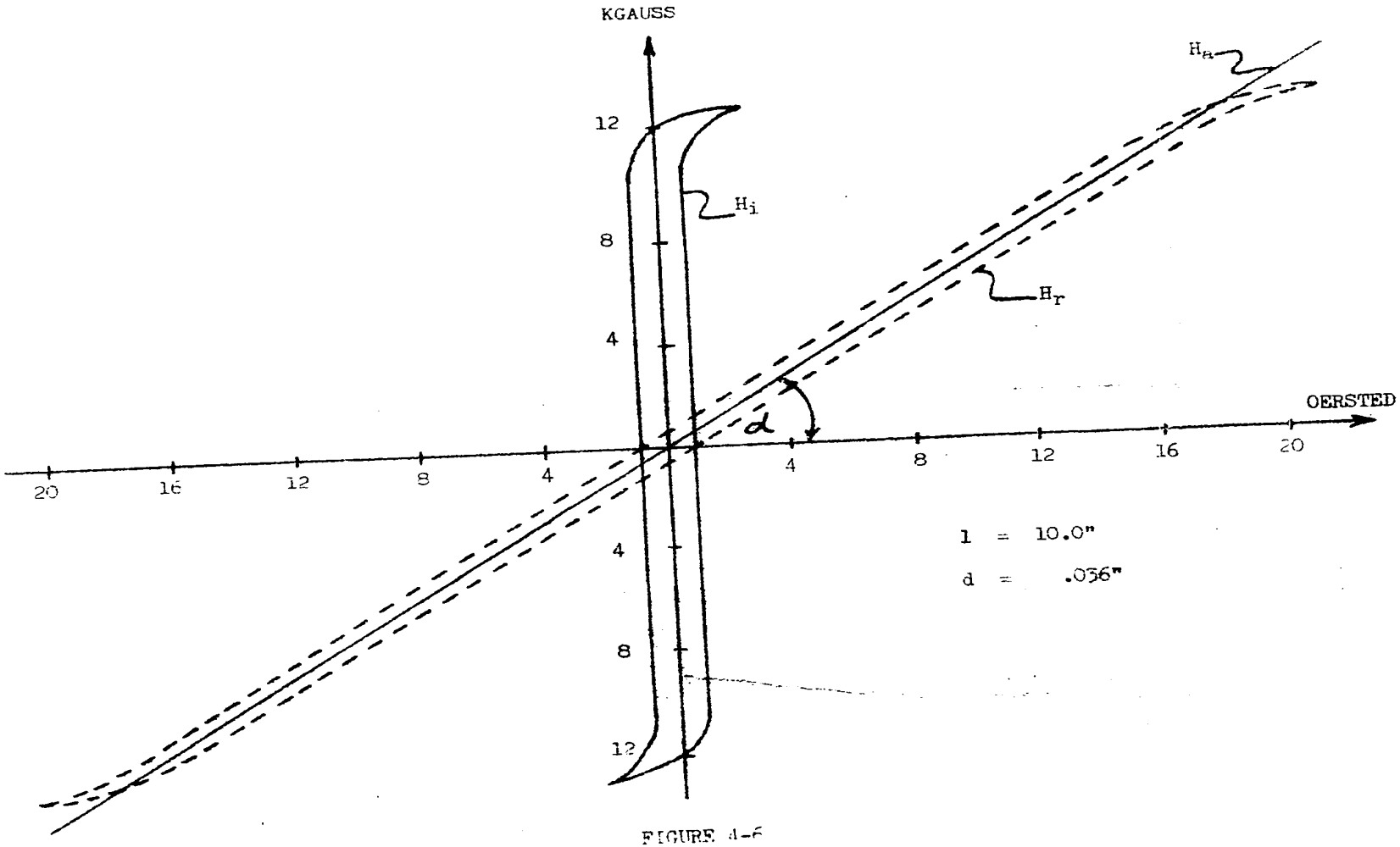
KGAUSS
12
8
4
4
8
12
H_i
H_a
H_r
d
OERSTED
20
16
12
8
4
4
8
12
16
20
l = 10.0"
d = .036"

FIGURE 4-6

Let us have a glance at the complete system, illustrated in fig. 4-7 by its block diagram. It must be remembered at this point, though, that everything is based on the principle that a cell is rewarded when, and only when, it fires or punished if it does not fire.

The blocks (1), (2), (3) and (4) describe the behaviour of the cell as outlined in chapter 2. The inputs are fed to a summing network and then go through an RC integrator; the output of this last block is compared to the threshold and, should it exceeds the threshold, the cell fires. For the present purpose, it will be assumed that the delay between the output of block (1) and of block (3) is 1 usec.; then the delay of block (5) shall be just over 1 usec.. The function of the separator is to decide if the pulse coming from the cell or from the delay should be impressed on the core. In other words, if the cell fires, the separator will act so as to impress this pulse on the core and to prevent the pulse coming from the delay from reaching the core. If, on the other hand, the cell does not fire, the separator will let the delayed pulse be impressed on the core. The block (7) of course reacts directly on the threshold in a direction determined by the state of the cell. It will be seen later how this can be realized practically.

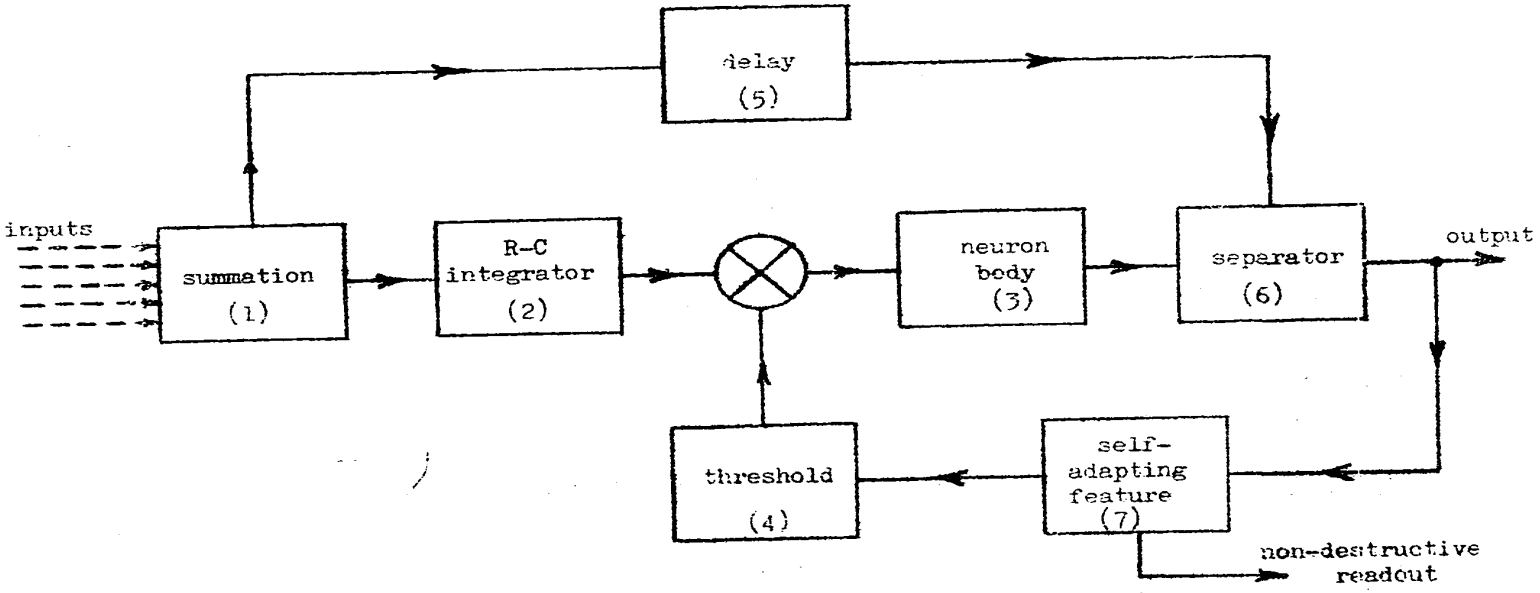

PROPOSED SELF-ORGANIZING NEURON

Figure 4-7

- CHAPTER 5 -

- PRACTICAL DEVELOPMENT -

PRACTICAL DEVELOPMENT

The air gap, as expected, makes some drastic changes to the hysteresis loop. It is therefore essential that means be found in order to minimize as much as possible these effects. It will be seen, in the present chapter, how the best materials for both the Hall element and the core can be selected. The magnetic properties of the cores will be first looked into.

5-1. Magnetic Properties.[31,35]

The important magnetic properties are the coercive force, the peak flux density and the residual flux density. The coercive force H_c is the value of the reverse intensity needed to produce a condition of zero flux density. The peak flux density B_s is the flux density of the specimen when the field strength has been sufficient to magnetize the material practically to saturation, while the residual flux density B_r is the value of flux density when the field has been reduced to zero, after having reached saturation. The ratio of these last two terms, i.e. the ratio of the residual induction to the induction at saturation, is usually referred to as the squareness factor;

$$R_s = \frac{B_r}{B_s} \qquad (5\text{-}1)$$

Different cases illustrating the effects of an air gap on cores having different values for the peak flux density and the coercive force are

shown in fig. 5-1. The length of the magnetic path is considered to be 10 inches while the width of the air gap is 0.002 inch. The squareness factor remains the same throughout and is taken as 0.9.

The important factor in all the resultant curves is the degree of shearness of the hysteresis loop. It is observed that the specimens a and b, c and d, e and f have identical maximum flux densities while the coercive forces vary. Vertically, (looking at the specimens a, c and e, or b, d and f) the situation is reversed, i.e. the magnetic fields stay fixed but the flux densities vary.

Some interesting facts can be extracted from the illustrations. It appears, first, that an increase in the maximum flux is accompanied by a larger degree of shearness. It is also noted that a larger coercive force minimizes the effect of the air gap.

5-2. Practical Criteria.

The above observations seem to imply that the flux density should tend to zero while the magnetic field should approach infinity. However, practical facts tend to modify these statements. Since the Hall voltage is proportional to the induction, the minimum value acceptable from a core is limited by the sentivity of the Hall element; B_m should be around 5 kilogauss for the commercially available elements. A second thought directs the consideration to the fact that the excitation

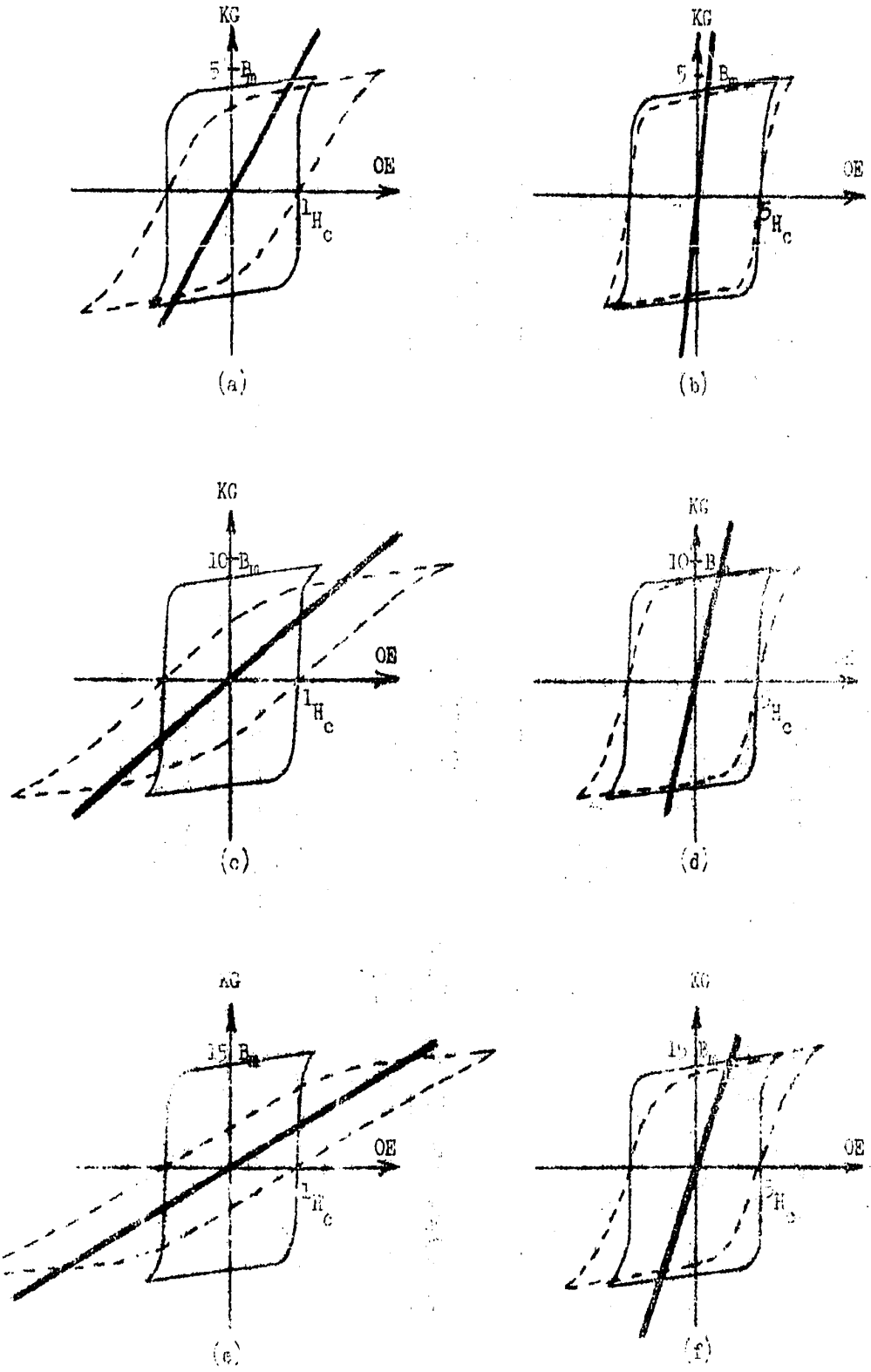

Figure 5.1

of the core becomes more and more difficult as the coercive force gets larger.

In other words, three criteria are presently available for the selection of the material; they are:

1. a large coercive force, say between 2 and 5 oersteds;
2. an average flux density around 5 kilogauss;
3. a squareness factor better than 0.80; this is a direct indication of the shape of the hysteresis loop.

5-3. Form and Selection of Core.

A quick look at the commercially available materials (see table 1) indicates that the ferrites seem the most appropriate for our purpose; we are particularly referring here to those materials called ferroxcubes commercially. In general, they consist of alloys like copper-zinc, manganese-zinc, nickel-zinc, manganese-magnesium, and others. However, due to the difficulty of obtaining ferrites with the desired characteristics, experiments have been conducted on an orthonol core, 50-50 nickel-iron, before a suitable ferrite core, (a beryllium ferrite) was obtained. The experiments have consequently been run on both types of cores.

As far as the form of the cores is concerned, it seems evident that toroids should be preferred to C or E/I cores since

TABLE I

	ELEMENTS	COMPOSITION %	H_c OE	B_s KGAUSS	B_r KGAUSS	$R = \frac{B_r}{B_s}$	u_i Kg/OE	u_m Kg/OE
Magnetic Iron	Fe	99.98	0.05	21.5	13.6	.633	25	275
Sendust	Fe,SiAl	85,9.5,5.5	0.05	10.0	5.0	.500	30	120
78.5 Permalloy	Ni,Fe,Mn	78.5,20.9,0.6	0.05	10.7	6.0	.560	9	105
Hipernik	Fe,Ni	50,50	0.06	15.0	7.5	.500	6	90
Mumetal	Ni,Fe,Cu,Mn	74,20,5,1	0.05	8.5	6.0	.706	7	80
4-79 Mo-Permalloy	Ni,Fe,Mo,Mn	79,16.4,4,0.6	0.05	8.5	5.0	.588	22	72
High-Silicon Steel	Fe,Si	95.5,4.5	0.5	19.0	5.0	.263	.750	8.3
Low-Silicon Steel	Fe,Si	99,1	0.7	21.0	8.5	.405	.350	5.2
Permendur	Fe,Co	50,50	2.0	24.5	14.0	.571	.800	5.0
7-70 Perminvar	Ni,Fe,Co,Mn	70,22.4,7,0.6	0.6	12.5	2.4	.192	.850	4.0
45-25 Perminvar	Ni,Fe,Co,Mn	45,29.4,25,0.6	1.4	15.5	3.3	.213	.213	1.8
Cast Iron Annealed	Fe		11.0	16.0	5.5	.344	.125	0.3
Deltamax	Fe, Ni	50,50	0.1	14.5	13.7	.945	1.0	110
Supermalloy	Mo,Ni,Fe	4,79,17	0.006	7.1	4.7	.662	87	600
Orthonol	Fe,Ni	50,50	0.1	14	13.0	.931	4	70
Supermendur	V,Fe,Co	2,49,49	0.26	24	21.15	.88		66
Ferroxcube 1	Cu,Zn	40,60					1.100	
Ferroxcube 2	Mg,Zn						.400	
Ferroxcube 3	Mn,Zn,Fe	45.5,49.5,5	0.1	2.50			1.000	1.5
Ferroxcube 4	Ni,Zn	40,60					.100	
Permenorm 5000Z	Fe,Ni	50,50	0.3	15.00			.500	40.0

Data chiefly extracted from references 31 and 36.

H_c = coercive force

B_s = peak flux density

R = squareness factor

B_r = residual flux density

u_m = typical maximum permeability

u_i = typical initial permeability

these last two types effectively increase the air gap with the one at the butt joint.

5-4. Core Construction and Air Gap Insertion.

The orthonol core is a tape wound core. This tape core is wound from a continuous strip of material (ref. fig. 5-2) with the last turn spot welded to hold it in place, where the penetration of this spot weld is limited to two or three outside laminations. Inner laminations are either left unfastened or are taped in place. This is then cased in a phenolic box for protection.

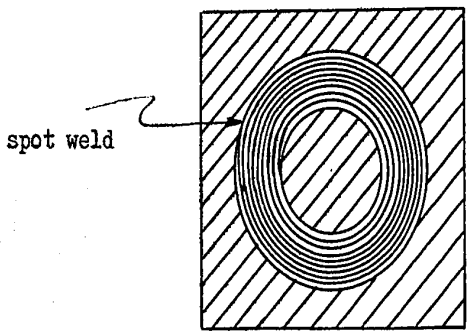

Figure 5-2

The thickness of the lamination is one mil (.001 inch) and consequently it is not easy to insert an air gap. The distance separating two laminations is also very small. It is not possible to cut the core directly since the spring force of the laminations would displace them against each other, then destroying the air gap.

Figure 5-3 illustrates the core after having

been cut and wound with the necessary number of turns. The first step, in order to produce an air gap, is to expose the laminations on both lateral sides by removing part of the proctective casing. A liquid cement is then heated so that its viscosity is reduced and slowly poured in between the laminations. This is then permitted to solidify before a layer of resin epoxy, about 1/16 of an inch thick, is applied; this last process gives the core more resistance against the pressure of the saw. A diamond saw *) is then used to cut the gap of the desired thickness. This saw is effectively a grinding wheel turning at a very high speed.

The second specimen is a beryllium ferrite. Ferrites are prepared by a sintering process as commonly used in the ceramic industry. The metal oxides, carbonates or other compounds which are to form the ferrite by a chemical reaction, are mixed homogeneously and wet-milled. The dried powder (which may or may not have been pressed into a particular shape) is prefired at a high temperature in order to bring about the initial chemical reaction between the constituents. To obtain a chemically homogeneous sample, the prefired powder is again milled and mixed. This powder, after the addition of a binder, is pressed into the required shape. The pressed product is again sintered at a temperature determined by the desired properties of the ferrite.

Ferrites are not entirely dense materials; they have a certain porosity on which depends their mechanical strength. They

*) The author wishes to acknowledge the technical as well as experimental assistance of the Northern Electric Co. Ltd in Ottawa to perform this operation.

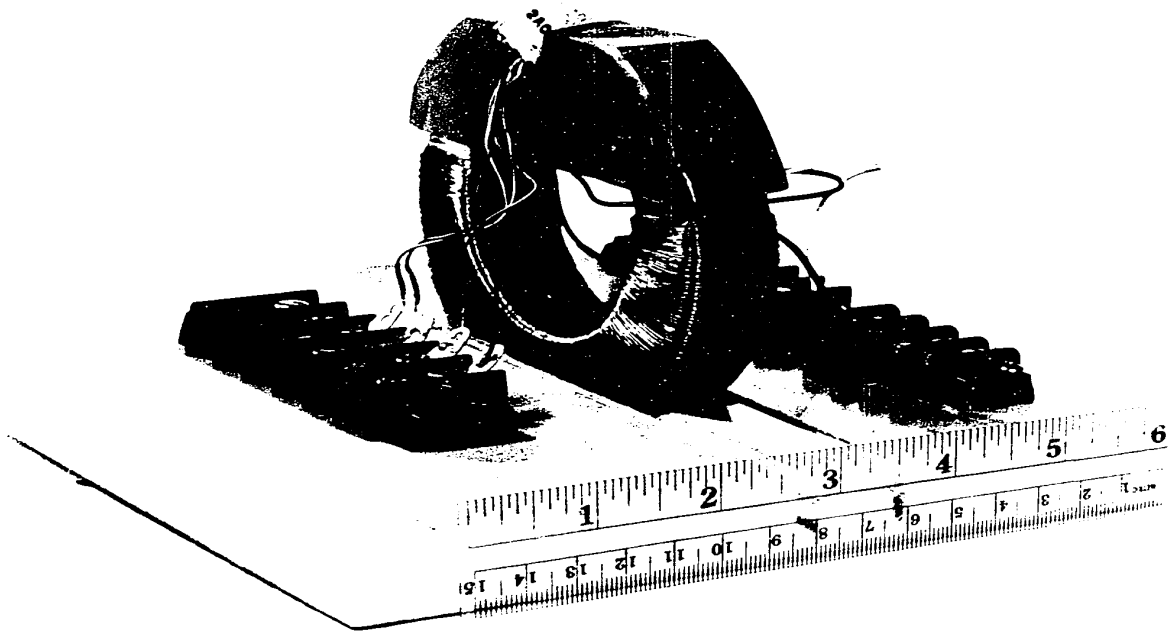

cannot be worked with a cutting tool, but can be ground or lapped. The same diamond saw, used for the orthonol core, was utilized to insert the air gap in the ferrite core. Means were taken to reduce the lateral pressure exerted by the saw. Once the air gap of the proper thickness was obtained, the Hall element was inserted and cemented in place.

5-5. Characteristics of Cut Cores.

The magnetic properties of the cores, once the air gap has been introduced, are changed according to the explanation in chapter 4. The shape of the hysteresis loop for both the uncut and cut cores, was found by means of the circuit shown in fig. 5-3.

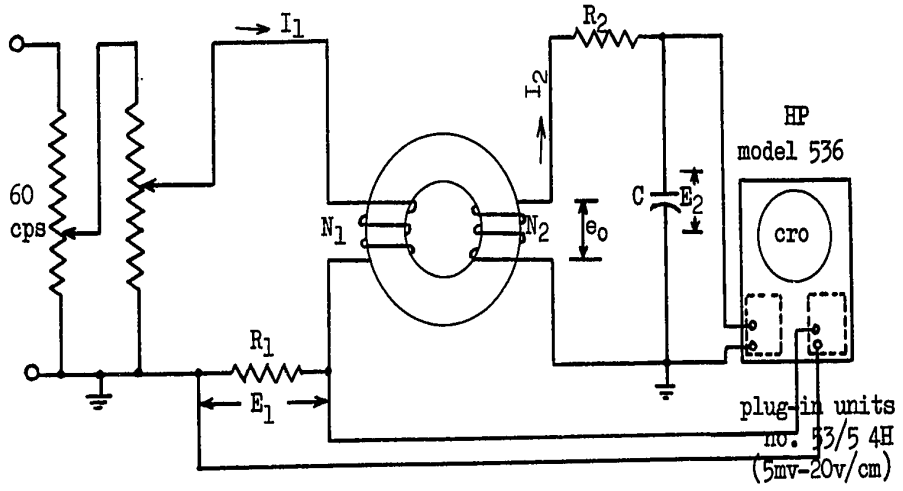

Figure 5-3

The magnetic field in the specimen is given by:

$$H = \frac{N_1 \cdot I_1}{\ell} \text{ at/m} \qquad (5\text{-}2)$$

where ℓ = length of the magnetic path in meters.

now, since $I_1 = \frac{E_1}{R_1}$

then: $$H = \frac{N_1 \cdot E_1}{\ell \cdot R_1} \text{ at/m} \qquad (5\text{-}3)$$

Converting the units of magnetic field from at/m to oersted, since

$$1 \text{ oersted} = 79.6 \text{ at/m}$$

we get: $$H = \frac{N_1 \cdot E_1}{79.6 \cdot R_1} = 1.255 \times 10^{-2} \frac{N_1 \cdot E_1}{\ell \cdot R_1} \qquad (5\text{-}4)$$

E_1, R_1 and N_1 are chosen to suit the specimen under observation. The only limitation is that R_1 should be smaller than the resistance R_{w1} of the primary winding so that R_1 does not load the source too much.

To obtain an indication of the flux, an integrator circuit is needed, since:

$$e_o = N_2 \frac{d\phi}{dt} \qquad (5\text{-}5)$$

An R-C network performs the necessary integration if the R-C time constant is chosen so that:

$$\frac{1}{wC} \ll R \qquad (5\text{-}6)$$

This can easily be shown by analyzing the circuit.

$$I_2 = \frac{e_o}{R_2 + j\left(wL - \frac{1}{wC}\right)} \qquad (5\text{-}7)$$

where L is the inductance of the secondary winding. The resistance R_w2 of the secondary winding is neglected since it is much smaller than R_2. (6-5) in (6-7) yields:

$$I_2 = \frac{N2\ d\phi/dt}{R_2 + j\left(wL - \frac{1}{wC}\right)} \qquad (5\text{-}8)$$

Now, $wL \ll \frac{1}{wC}$ and can therefore be neglected. If, on the other hand, the condition expressed by eq. (5-6) is met, then:

$$I_2 = \frac{N_2\ d\phi/dt}{R_2} \qquad (5\text{-}9)$$

Consequently, the voltage impressed on the capacitor C is given by:

$$E_2 = \frac{1}{C}\int I_2\ dt$$

$$= \frac{1}{C}\int \frac{N_2}{R_2}\frac{d\phi}{dt}\ dt$$

$$= \frac{1}{C}\int \frac{N_2}{R_2}\ d\phi$$

$$\therefore \quad E_2 = \frac{N_2}{R_2 C}\cdot\phi \qquad (5\text{-}10)$$

where ϕ is in webers.

To express the flux density in terms of kilogauss, the transformation of

units is required;

$$\phi = BA \qquad (5\text{-}11)$$

where A is the cross-sectional area of the core in m^2. ; then eq. (5-10) becomes :

$$B = \frac{R_2 C}{N_2 A} E_2$$

where B is in webers/$meter^2$;

since $1 \text{ weber/meter}^2 = 10 \text{ kilogauss}$

$$B = 10 \frac{R_2 C}{N_2 A} E_2 \qquad (5\text{-}12)$$

Again R_2, C and N_2 are chosen to suit the core under investigation.

For the case of orthonol core, the physical dimensions are :

I.D. = 2.5"

O.D. = 3.5"

h = 0.5"

As a consequence :

ℓ = 23.71 cms

A = 1.210 cm^2

The following values are then selected :

N_1 = 500 turns (gauge no.30 AWG)

R_1 = 1 ohm

N_2 = 100 turns

R_2 = 1 megohm

C = 0.1 microfarad.

From eqs (5-4) and (5-10), the relations for B and H are obtained :

$$H = 1.255 \times 10^{-2} \times \frac{500}{0.2371 \times 1} E_1$$

and

$$H = 26.5 \; E_1 \; o_e. \qquad (5\text{-}13)$$

$$B = 10 \frac{0.1 \times 10^{-6} \times 10^{6}}{100 \times 1.210 \times 10^{-4}} E_2$$

and

$$B = 82.7 \; E_2 \text{ kgauss.} \qquad (5\text{-}14)$$

Figure 5-4a shows the hysteresis loops for the toroid with and without an air gap of .036", as appearing on the oscilloscope. Figure 5-4b illustrates the loops once the transformations to magnetic units are performed. It is observed that the residual flux density is reduced from 12 kilogauss to just about one kilogauss. The coercive force, of course, does not change but the force required to reach saturation, H_m, increases to about 19 oersteds.

The second specimen is the ferrite. From the physical dimensions again, ℓ and A can be calculated.

I.D. = 1.0"

O.D. = $1\frac{5}{8}$"

h = $\frac{5}{16}$"

ℓ = 10.5 cms

A = .655 cm^2

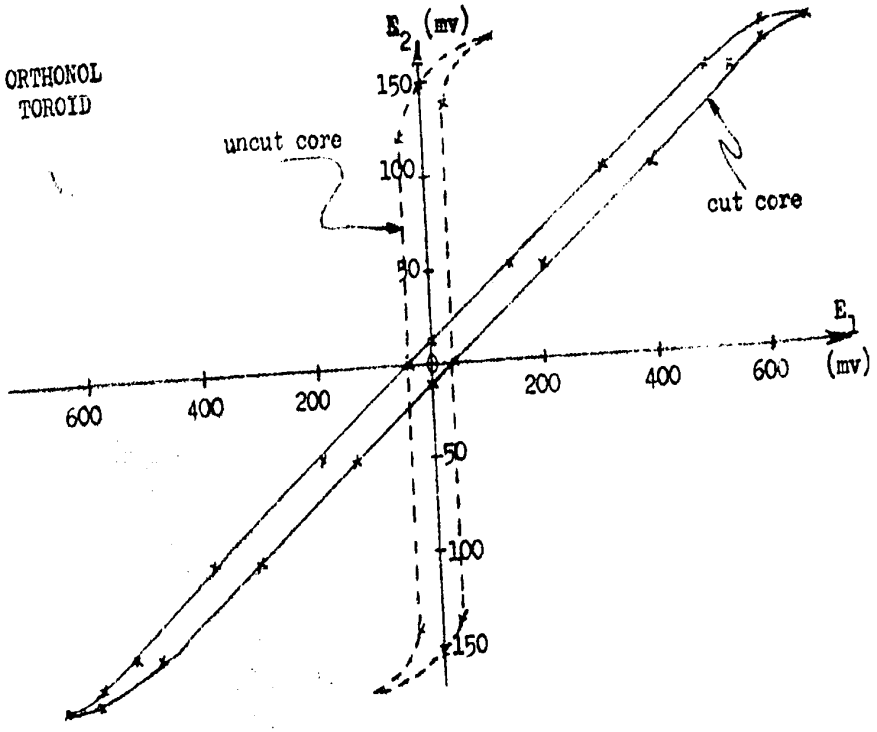

Figure 5-4a

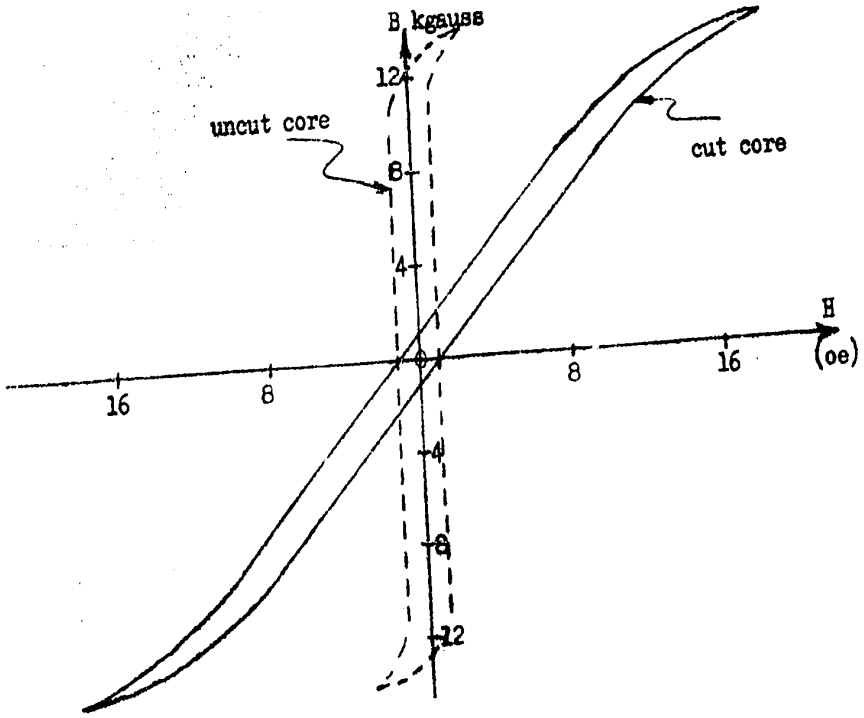

Figure 5-4b

It is now possible to select proper values for the elements of our circuit :

N_1 = 100 turns (gauge no.30 AWG)

R_1 = 1.1 ohm

N_2 = 100 turns

R_2 = 320 kilohms

C = 1 microfarad

Utilizing again eqs. (5-4) and (5-10), the relations for B and H are obtained :

$$H = 1.255 \times 10^{-2} \times \frac{100}{0.105 \times 1.1} E_1$$

and

$$H = 10.85 \; E_1 \qquad (5\text{-}15)$$

$$B = 10 \; \frac{320 \times 10^3 \times 1 \times 10^{-6}}{100 \times .655 \times 10^{-4}} \; E_2$$

and

$$B = 489 \; E_2 \qquad (5\text{-}16)$$

The oscilloscope traces and their transformations appear in fig. 5-5a and 5-5b. As in the case of the orthonol, the shearing is pronounced, although the width of the air gap, this time, is .050" due to the fact that the particular Hall element intended for this toroid has such a thickness.

Comparing fig. 5-4 and 5-5, though, it is seen that the ferrite core, for a larger air gap, gives much better results than the orthonol toroid; to strengthen this argument, it will suffice to quote the squareness ratio of both cut cores :

Ferrite : $R_{sf} = \frac{300}{1,550} = 0.194$

Orthonol : $R_{so} = \frac{1000}{14,000} = 0.071$

Although this yields an improvement in ratio of about 3:1, these results do not seem sufficient to even prove that the proposed model would work. It is understood, of course, that it is only intended, at this stage, to prove the principle; improvements should come later. The only way left to get better results consists in a judicious choice of the Hall element.

5-6. Commercial Hall Elements.

Of all the commercially available Hall elements, two types were selected. Their physical characteristics along with their sensitivity are shown in fig. 5-6. The one on the left, the Halltron HR-31 from Ohio Semiconductors, utilizes a thin wafer of Indium Arsenide (InAs) vacuum deposited between two pieces of ceramic/glass. This is then covered with a proctective coating of resin. The dimensions of the semiconductor strip are :

length : 0.250"

width : 0.125"

thickness : 0.005"

The one on the right is the Hallefex 335 from Helipot Division of Beckman Instruments Inc. and consists of a slab of Indium Antimonide (InSb) inserted

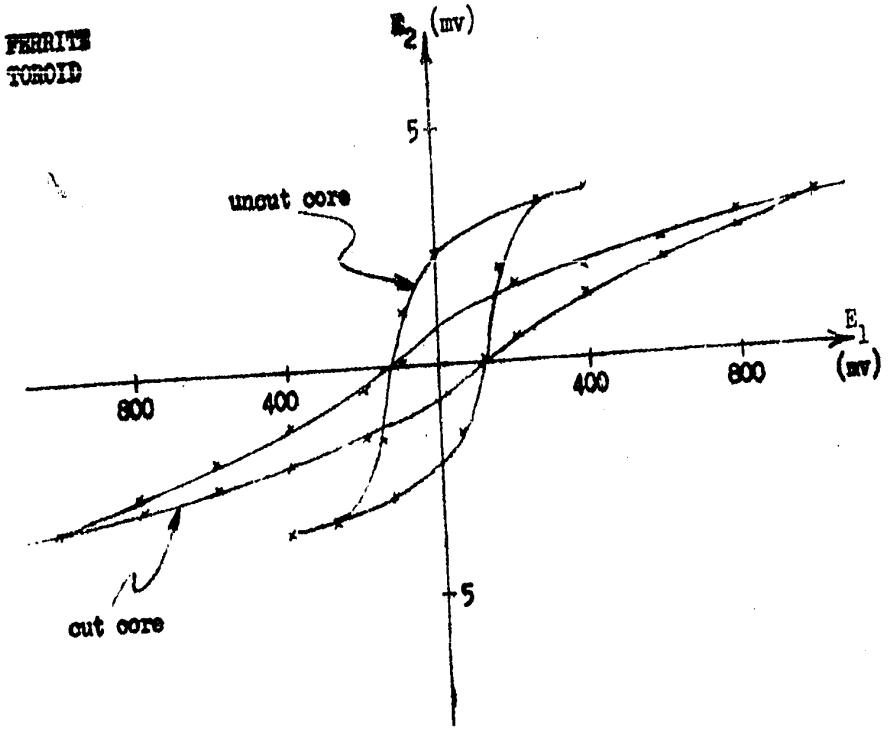

Figure 5-5a

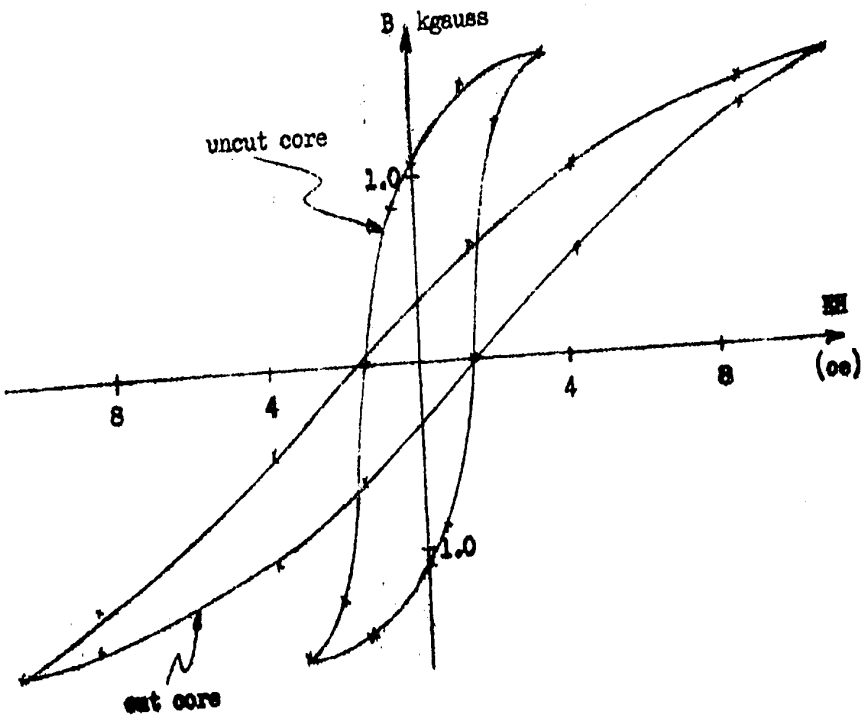

Figure 5-5b

between two ferrite pieces. The dimensions of the active element are :

length : 0.200"

width : 0.060"

thickness : 0.002"

The main advantage of the Hallefex 335 is that the two ferrite pieces have the effect of reducing the effective air gap to just a little more than the film thickness. Theoretically, the effect[37,39] on the B-H curve can be derived in a manner similar to the case of the iron and air gap in series, found earlier in chapter 4. The only difference in the expression for the magnetomotive force is in the addition of a third term due to the ferrite strip. The m.m.f. is then expressed as :

$$F = l \left[H_i + H_a \frac{d}{l} + H_f \frac{p}{l} \right] \qquad (5\text{-}17)$$

where H_f is the magnetic field in the ferrite,

p is the total thickness of the ferrite strips.

Figure 5-7 gives a picture of all the components while figure 5-8 is a graphical representation of the new hysteresis loop as given by the above equation.

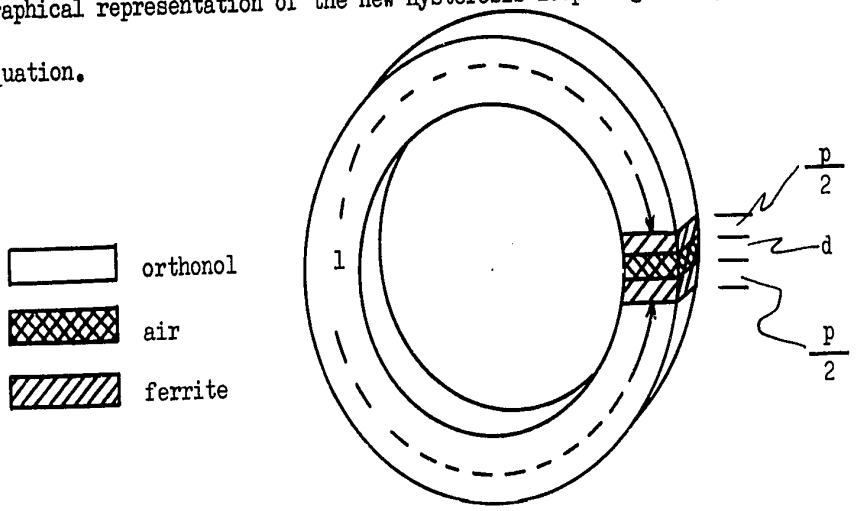

Figure 5-7

HALLTRON HR-31

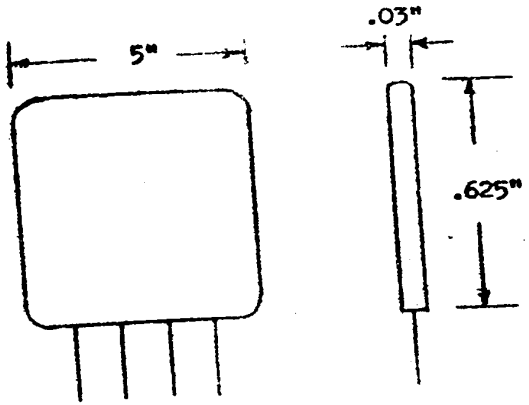

HALLEFEX 335

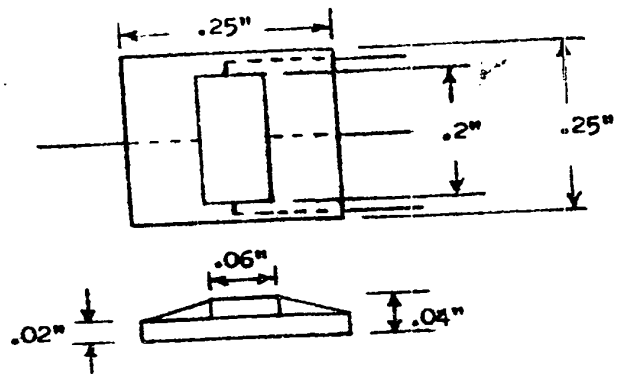

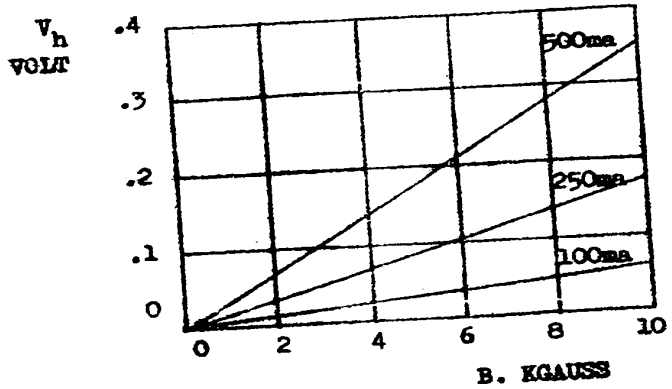

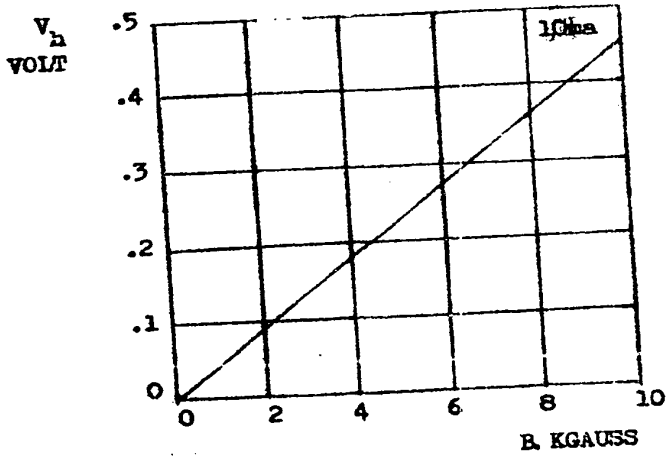

Figure 5-6

It should be noted, however, that this is possible by assuming that the hysteresis loop of the ferrite is known; in other words, the B-H curve of a ferrite toroid with the same physical dimensions as the core under investigation is known. For the case shown, the core is the orthonol toroid and the air gap is taken as being just the thickness of the strip of InSb in the Hallefex 335. This is of course theoretical. The effective results obtained in practice will be shown in the next chapter.

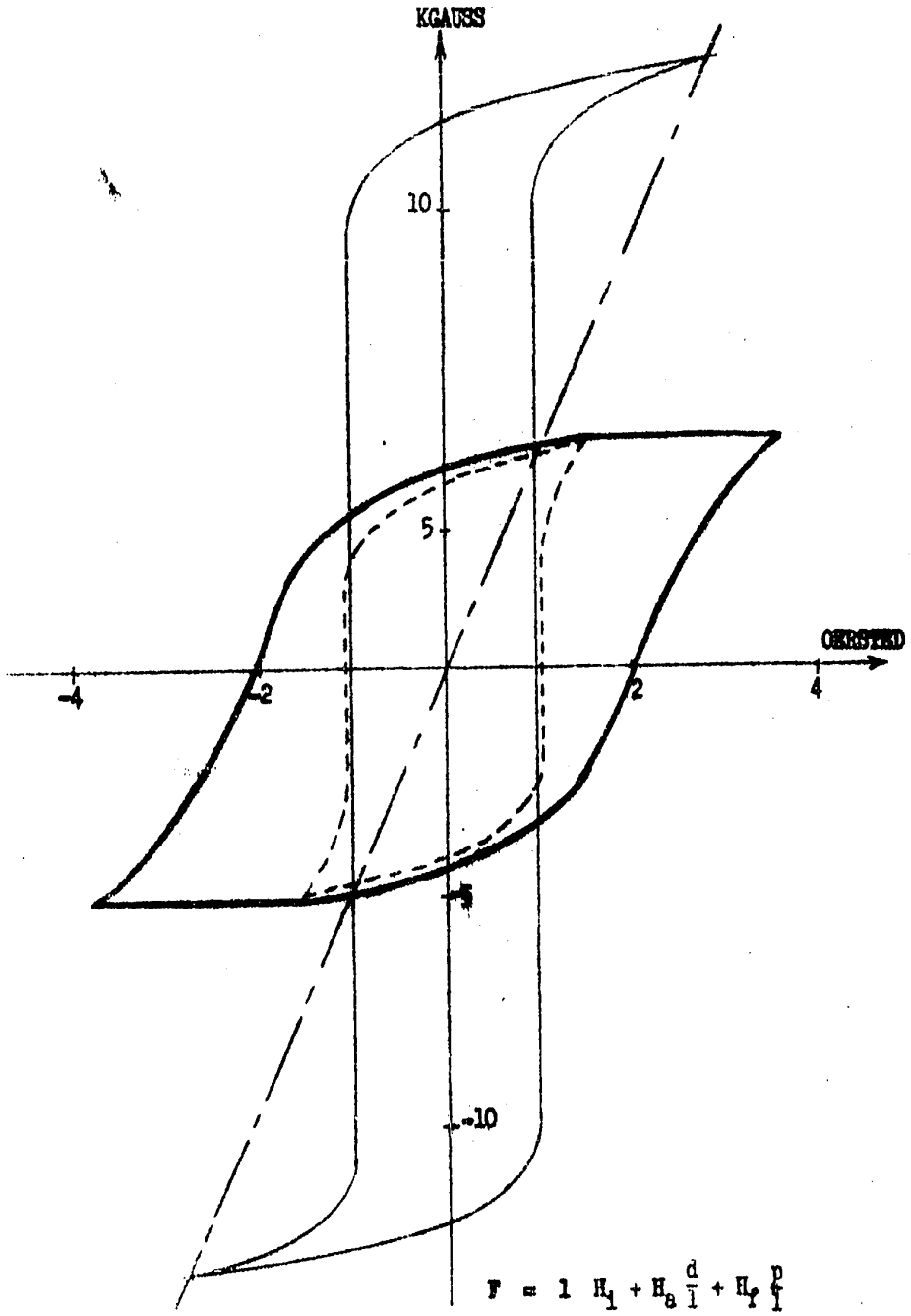

Uncut toroid

Air gap

Effective ferrite

Resultant

- CHAPTER 6 -

- RESULTS -

RESULTS

As outlined earlier, to obtain states on a specific core seems rather an easy matter if the conditions set forward are met. However, to explain the theory and to get the expected results practically are two different things. When someone talks about some theoretical principle, he obviously does not considers the secondary effects which appear when working with actual components. A perfect capacitor or a perfect inductor does not exist as such. For one thing, there is always some resistance attached to such an element. In order to follow more closely the progress and development of the present system, it will be shown first how states can be obtained on an uncut toroid; from there, it should be an easy matter to proceed to the case of the core with an air gap. As a matter of fact, this was also the procedure followed in the theoretical part.

States on an Uncut Core.

The specimen used for this case is also an orthonol toroid. It is slightly different, physically and magnetically, from the one described earlier, which was cut in order to insert an air gap. It has the following dimensions :

I.D. = 3.0"

O.D. = 3.5"

h = 0.5"

The hysteresis loop is illustrated in figs 6-1a and 6-1b.

It has been shown before that the increment in flux on a core is given by the relation:

$$B = 10 \frac{E \cdot \Delta T}{N \cdot A} \quad \text{kilogauss} \qquad (6\text{-}1)$$

where ΔT is the width of the pulse in seconds. The other symbols are as defined earlier. In order to impress identical "volt-time" area pulses on the toroid, one immediately thinks of a pulse generator. However, this instrument has a very high output impedance - 5000 ohms - compared to the impedance of the winding; the resistance of 50 turns of gauge no. 30 (AWG) is about 1 ohm. The transfer of energy is consequently negligible. Similar conditions result when the output of an electronic neuron drives the core; it is known that these neurons have standard 12 v., 4 msec. pulses as outputs.

Another idea for the proper excitation is to use an emitter follower; the only limitation here seems to reside in the fact that the intensity of current to which the core is subjected depends on the d.c. source and on the type of transistor. This, then, does not represent any problem if a judicious selection is made of the type of transistor along with the proper d.c. source. This circuit - without R_g and R_o - is represented in fig. 6-2. A rectangular voltage pulse, with spikes, is however obtained across the winding; the amplitude of the spikes is much greater than the voltage amplitude of the pulse itself and, as a consequence, is

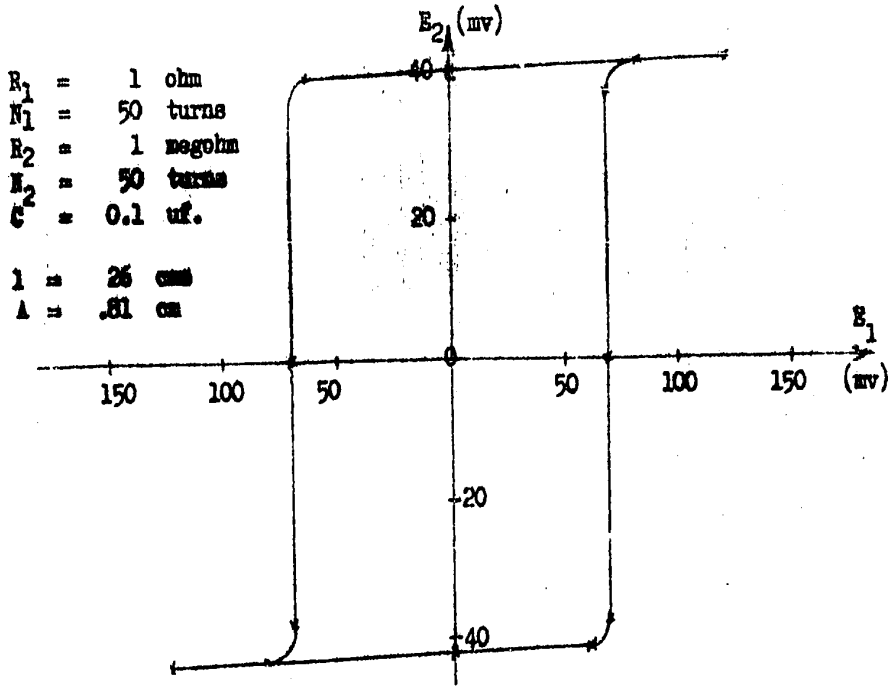

Figure 6-1a

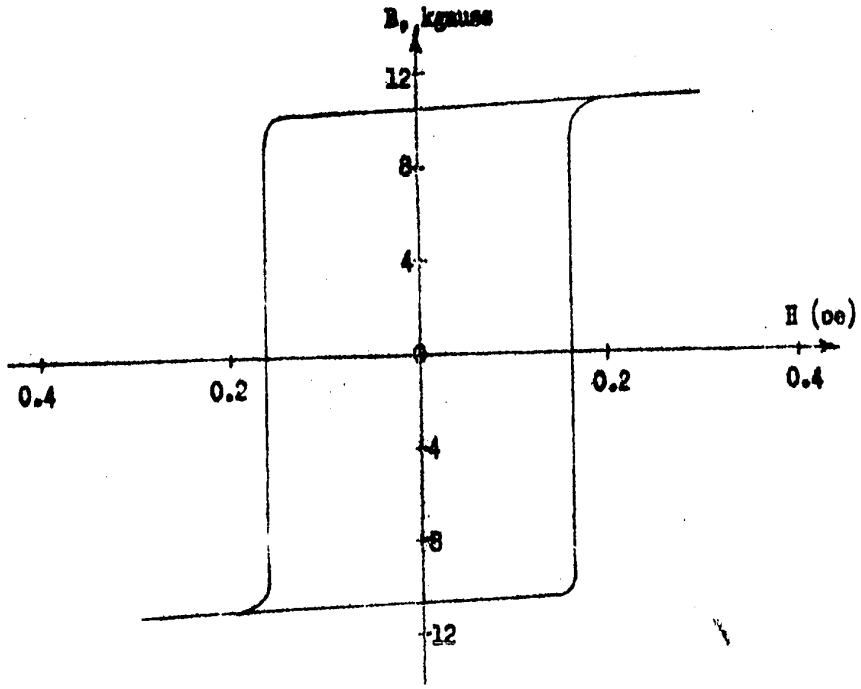

Figure 6-1b

sufficient to send the core from positive remanence to the negative one, or vice-versa depending on the polarity of the spike. Since each pulse is accompanied by two spikes of opposite polarity, the flux goes around the loop once for every pulse.

The origin of spikes is in the rate of change of current with respect to time; the pulse generator has a rise time of 0.5 usec. and, since the switching time of the transistors used - Philco 2N224's - is better than that figure, it means that the voltage across the inductor is tremendous when the pulse rises and falls down to zero. A resistance R_o, is inserted in parallel with the inductor to cure the undesired effects of the spikes; it effectively limits the amplitude of voltage that can appear across the winding. Of course, the intensity of the spikes decreases as R_o is made smaller and smaller but there is a point where the intensity of the spike is no longer prejudicial. Different values for R_o are obtained for different cases, where each case is determined by the number of turns on the primary winding and by the "volt-time" area of the pulse across this winding.

Now, once the desired waveform is impressed across the core, this does not mean that this waveform is effectively across it since there is a series resistance also present. It is an R-L circuit as shown in fig. 6-3; the responses to a step input of 1.0 are also illustrated for different values of the time constant R/L. The horizontal axis is time, but it is to be remembered that the pulses dealt with, from the

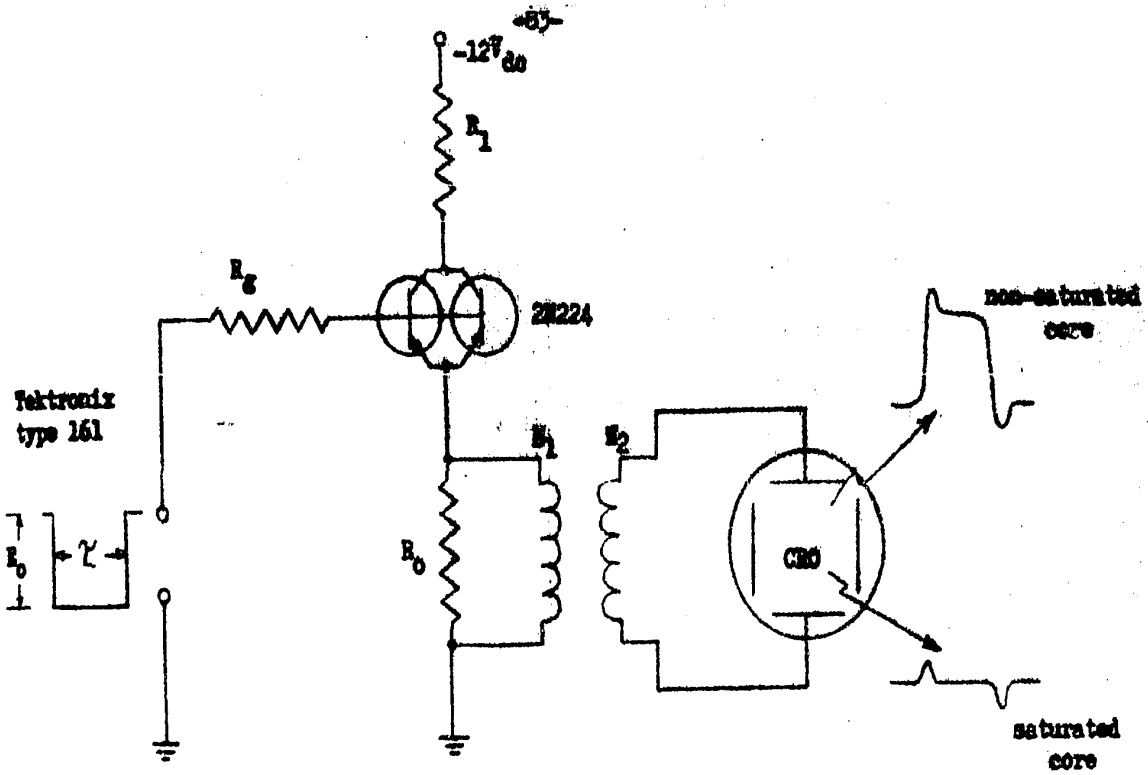

DRIVING CIRCUIT

Figure 6-2

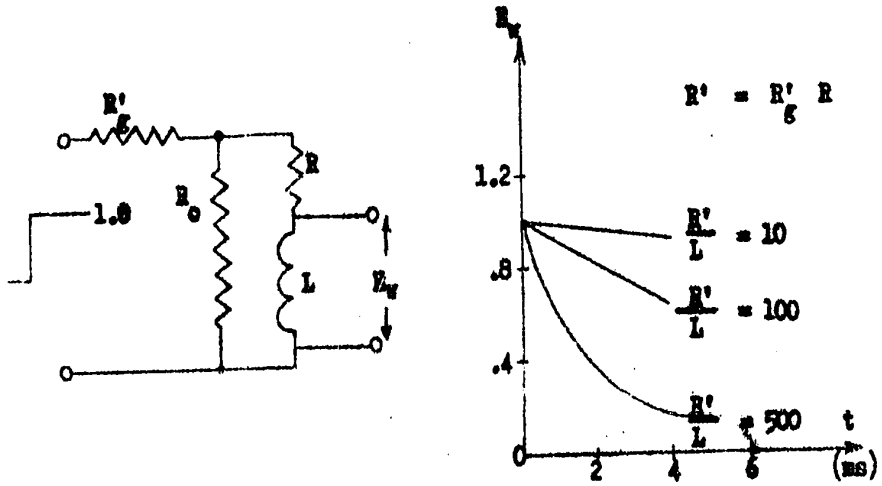

Figure 6-3

neurons, have a width of 4 msec.

It is seen that R/L should be as small as possible; R'_g is the effective resistance of R_g when in the emitter circuit:

$$R'_g = \frac{R_g}{40} \qquad (6\text{-}2)$$

were 40 is roughly the current amplification factor of a 2N224. It should be noted that R_o has another role now; increasing R_o adds weight to R'_g and distorts the waveform across the core. A larger R_g, on the other hand, limits the current to the base of the transistor and consequently reduces the amplitude of the same waveform. But R_g is one of the means of varying ΔB, as expressed by equation (6-1), in order to increase or decrease the number of states.

Now that the driving circuit has been cleared of difficulties, comes the time when the assembly should be made to work. In table II are listed the results for the specimen discussed. If a secondary winding is added to the core, then the voltage induced in it is as shown in fig. 6-2. The important factor is of course the voltage across the primary winding; it is a function of the emitter current which in turn has a direct relation to the base current. Since Rg and E_o control the base current, it is not necessary to vary both E_o and R_g. Since the emitter to ground impedance looks much larger on the input side, it seems that R_g should be the variable parameter.

Table II

R_g kohm	R_o ohm	E_o volt	E_w, (mv)		E_{cro}, (mv)			States no.
			pulse	spike	non-satur. pulse	non-satur. spike	satu-rated	
0	.23	-30	140	40	240	60	100	30
2.2	.23	-30	130	10	50	25	70	50
4.4	.23	-50	100	20	40	15	70	65
10	.23	-50	65	15	30	40	55	125

$N_1 = N_2 = 50$ turns

R_g = series resistance in the base of transistor,

R_o = parallel resistance across core winding,

E_o = pulse amplitude from pulse generator,

E_w = " " across the core,

E_{cro} = pulse induced in the secondary winding of the core

spike = voltage amplitude of the spike

States no.= number of steps that the core goes through when driven from one remanent position to the opposite one

A few observations need to be made about these data. First of all, a decrease in the amplitude of the pulses applied to the core increases the number of states. However, from above, it seems that

the number of states is not directly proportional to the pulse amplitude; in the present case, this is true if the effects of the spikes are neglected, but if they are not, then the equation still holds. There is very little fallback and this cannot account for very much in the discrepancies noted above. The electronic Counter/Timer from Marconi Instruments Limited, type TF922/2, was used to take these readings. It was also noted that the increments in flux from one state to another were fairly equal, except for the last few states where the increments were progressively decreasing towards zero. This is in accordance with fig. 6-1b where the B-H curve, starting for instance from negative remanence, is almost vertical until saturation is approached. At that point, severe nonlinearities occur and these cause the decrease in flux mentioned above.

Cut Cores.

a. Orthonol Core.

For the cut toroids, two different cases present themselves according to which one of the two Hall elements is used. Fig. 5-4 has previously shown the hysteresis loop of the orthonol core with an air gap. Since the Hall element HR-31 has a ceramic/glass coating, it does not affect the B-H curve.

As the field required to reach saturation is around 19 oersteds or 1520 amp.-turns/meter, this is the minimum field with which

one must drive the core to obtain the states properly. Consequently, 2000 turns of gauge no. 30 are wound around the core. The necessary current is then of the order of 200 ma.

There are two different ways to obtain a direct measure of the state of the core, as illustrated in fig. 6-4. Both are equally good, but the micro-voltmeter method might be preferable when the increment of flux is small. The same driving circuit as for the uncut toroid is set up. Measurements on the oscilloscope were first obtained; the waveform appearing on the oscilloscope did not change from one pulse to another but stayed the same for all the pulses. The reason was that, due to the high degree of shearing, the voltage induced for each driving pulse was very nearly equal, independently of the state of the core. The amount of flux due to the fallback was nearly equivalent to the amount of flux needed in the forward direction to bring a change of state of the core. This meant effectively that the increment of flux necessary to send the toroid from state "n" to the state "n+1" was almost equal to the amount of flux to go from negative remanence to positive remanence.

The second method was tried next; a d.c. current of 450 ma was sent through the Hall element and a micro-voltmeter was inserted between the output leads of the element. A warm-up period of half an hour was allowed before any data was taken. After that, the first thing noticed was that the Hall voltage for an induction of zero

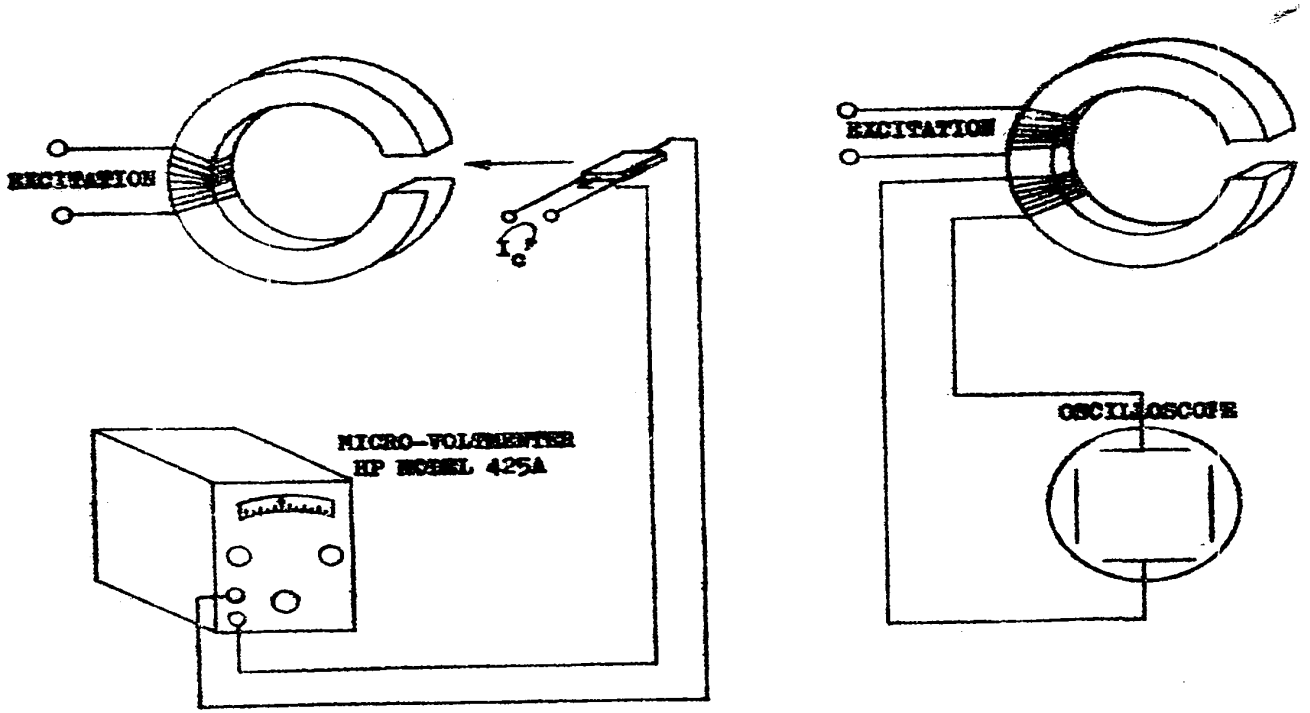

Direct Measurement of State of Core

Figure 6-4

was 6 mv.; the voltage at positive or negative remanence went up to + or -9 mv. respectively. It means that, if "n" states are desired, the indicator should change by 3/n for each state. This is rather small and difficult to observe within the limitations of the equipment. The driving pulses were then introduced with an amplitude sufficient to produce a field of 20 oersteds. Starting from negative remanence, - -9 mv. on the meter -, the first pulse sharply brings up the pointer to +150 mv. and down to +9 mv; oscillations around that value occur for succeeding pulses. Other attempts through a variation in the width or amplitude of the pulse were unsuccesful; the amplitude variation should be made by varying R_o. The series resistance of the inductor is 45 ohms and any value for R_o larger than 2.2 ohms prevents the transistors from delivering the necessary current; other switching transistors with higher current ratings could be used but, due to the characteristics of the circuit, they would need a collector voltage of abount 50 volts and very few transistors, if any, can operate at such a voltage. The cost at the same time would be extremely high.

The second type of Hall element, the Hallefex 335, was then inserted in the gap of the orthonol toroid. A circuit was set up to measure the new hysteresis loop; however, the characteristics did not show any change; instead, as saturation was approached a very strong vibration of the laminations occurred in such a way as to pull the laminations very close together, therefore destroying the gap and preventing the lines of flux to cross the semiconductor strip. The size of the element was not large enough to completely cover the laminations in order to prevent the

displacement. Both sections are illustrated below where the dimensions are enlarged to twice the actual physical dimensions. The hatched area is the area where the laminations were vibrating.

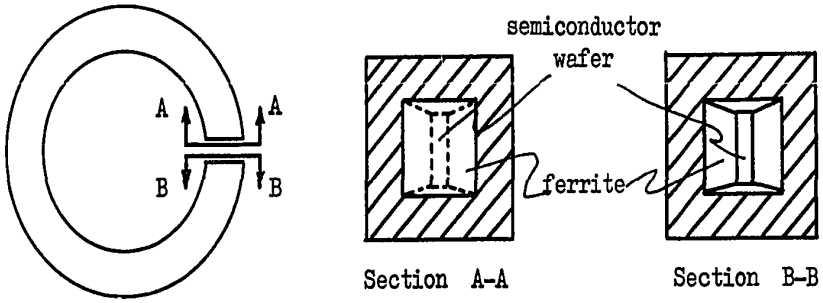

Figure 6-5

An improved process of cementing the laminations together when the operation of inserting an air gap was undertaken would have probably cured this defect. Nevertheless, it is believed that the results would not have been any better than the ones with the HR-31 when considering the fact that the size of the air gap had to be increased from .036" to .050" due to the larger thickness of the Hallefex 335.

b. Ferrite Core.

Once a gap of .050" is cut in the toroid, the specimen is very brittle and it is imperative that some spacer be inserted in this gap to prevent the core from being broken. Since the HR-31 does not improve the hysteresis loop while the Hallefex 335 does, and since a loop as square as possible is desired, this last element

was fitted from the beginning. After this was done, the cement was poured in between the element and the core in order to hold securely the assembly.

The same circuit as used for fig. 5-5 was then set up and the new magnetic characteristics were found. They are illustrated in fig. 6-6; the B-H curve of the core with the air gap alone is also shown for reference. Improvements are self-evident. The squareness ratio goes up to : $R'_{sf} = \frac{850}{1,550} = 0.55$ as compared to 0.194 when the element is not in. The degree of improvement, however, is not as good as expected from the theory. Several reasons could account for that; first of all, the manufacturer quotes 4 kilogauss as the saturating value for the ferrite coating of the element while the coercive force, which depends on the physical dimensions of the toroid, is of course not known; the squareness ratio is also unknown. A second point is that the surfaces of the Hall element are not exactly parallel as they should; measurements with a micrometer show that the thickness varies from .039" to .048"; the manufacturer quotes .040" with a thickness of .002" for the semiconductor strip. Since a margin of .002" was allowed in cutting the gap for safety purpose, it means that the air gap is actually about .012", roughly six times what it should be. Nevertheless, the results are still good enough to prove the principle.

Again the circuit of fig. 6-2 was set up. The micro-voltmeter method was utilized. It was observed that the residual

FERRITE TOROID

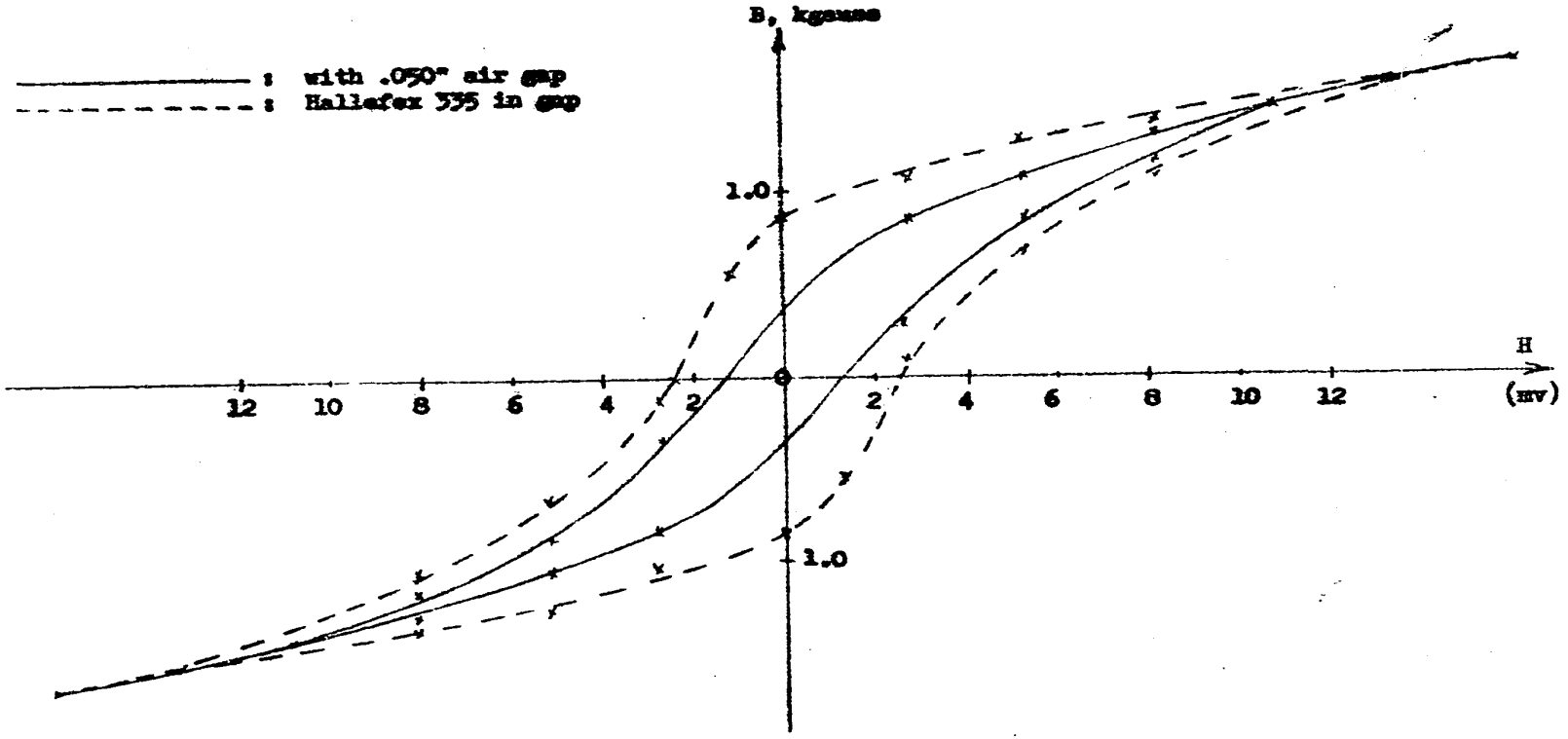

Figure 6-6

flux density produced a Hall voltage of 30mv. when a current of 10 ma flows in the input leads of the Hall element. R_1 was chosen as 7.5 ohms and, after several trials, it was found that a primary winding of 500 turns was the most satisfactory with respect to the present types of transistors. The negative effects of the spikes were best eliminated with a value of 4.4 ohms for R_o. Two parameters are then left for variation, that is R_g and E_o, the pulse amplitude at the source. Tables III and IV show the results when one parameter at a time was varied the other being held constant.

Table III shows the readings of the micro-voltmeter after each driving pulse when starting from remanence; the repetition of these pulses was set at 10 seconds so that the experimenter had ample time to take as accurate readings as possible. R_g was equal to zero and the pulse amplitude from the generator varied. The same period for the driving pulses was utilized in Table IV; this time however, the pulse amplitude E_o was kept constant at -40 v. while R_g was given different values between 0 and 10 kilohms.

The first observation noted in these results is the fact that the remanent point is not the residual flux density, i.e. that value of flux density when the field has been reduced to zero after having reached saturation. In other words, the exciting field has not reached H_m or saturation; the core then undergoes a minor loop. Even if this point is not really very important, it should be mentioned that this could be

Table III

E_o volts	Hall voltage mv.	Waveform impressed on core	States no.
-55	+17.5, -17.5, -19.0, -19.5 -19.0, +15.0, +17.0, +17.5	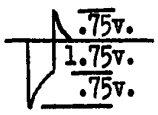	4 4
-45	-19.0, +15.0, +17.0, +17.5 +17.0, -16.5, -18.5, -19.0	" "	4 4
-35	-19.0, + 15.0, +16.5, +17.0 +17.0, -16.0, -18.0, -19.0	" "	4 4
-30	-18.5, +14.5, +16.5, +17.0 +17.0, -16.0, -18.0, -18.5	" "	4 4
-25	+18.0, -16.0, -18.0, -19.0 -19.0, +15.0, +17.0, +17.5	" "	4 4
-20	-18.0, +14.5, +16.5, +17.5 +18.0, -15.5, -17.5, -18.5	" "	4 4
-15	+18.0, -14.5, -17.0, -18.0 -18.0, +14.0, +16.0, +17.0	" "	4 4

NOTE: By number of states, is meant the number of steps that the core goes through when driven from one remanent position to the opposite one.

Table IV

R_g kohm	Hall voltage mv.	Waveform impressed on core	States no.
0.	see table III " " "	see table III	4 4
1.5	+15.0, -14.5, -16.5, -17.0, -17.5 -17.0, +12.5, +14.5, +15.0, +15.3	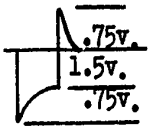	5 5
2.2	+16.5, -12.5, -14.8, -15.5, -15.8 -15.5, +12.0, +14.0, +14.8, +15.0	" "	5 5
4.7	-12.0, + 9.5, + 11.5, +12.0, +12.3 +12.0, -9.5, -11.5, -12.0, -12.3	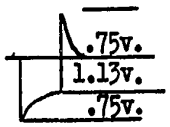	5 5
10.	+6.5, -6.5, -8.0, -8.5, -8.8 -8.0, +5.0, +6.5, +6.8, +7.0	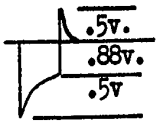	5 5

NOTE: By number of states, is meant the number of steps that the core goes through when driven from one remanent position to the opposite one.

corrected by utilizing higher current rating transistors. The second observation is that there seems to be a lack of symmetry with respect to the zero point; in both tables, the negative remanence produces a Hall voltage higher in amplitude than the positive remanence; the only reason is that the zero setting of the micro-voltmeter was not properly adjusted before the data were collected. The Hall d.c. voltage also accounts for part of this discrepancy.

Table III indicates that any value of E_o less than -15 v. for R_g = 0 ohm saturates the transistors i.e. the emitter current is completely independent of it. However for values between 0 v. and -15 v., the emitter current falls sharply, decreasing the Hall voltage and sending the core to other minor loops; this is deduced from the fact that the remanent points yield lower Hall voltages. Table IV on the other hand implies somehow the same conclusions; once R_g goes higher than 5 kilohms, the core switches to other minor loops as can be seen from the data but the number of states do not change; this last point is peculiar: the number of states should change with the intensity of the impressed pulses as implied in eq. (6-1); this condition however could only be met if the intensity of the spikes were taken care of at every new case. For R_g = 0 ohm, the height of the spike is 43% of the pulse amplitude while for R_g = 4.7 and 10 kilohms, this percentage goes up to 65%. If this ratio had been kept at 43, the number of states would go on increasing.

It is also noted that the increments in flux are

far from being equal. Since the characteristics of the Hallefex 335, as illustrated in fig. 5-6, give a straight line for the Hall voltage versus the induction, then equal increments in flux are reflected by equal voltage increments across the Hall element. If the present cases, where 5 states (or 4 increments) were obtained, are considered, then the following increments are observed on the average.

State number	Voltage increment, millivolts	Relative increment
1	29	100%
2	2	7%
3	0.5	2%
4	0.3	1%
5		

Relative voltage increments were calculated by considering the first increment as 100 and by taking the ratio of the other ones to the first. These of course refer to the degree of shearing of the hysteresis loop. Suggestions for improving the loop shape have been made earlier. The increments will tend to be equal as the B-H curve will tend to a perfect square. However, at this stage, our intention was only to show that the scheme proposed would work in principle and it is believed that this has been achieved. When our assembly is inserted in block (7) of fig. 4-7, a self-organizing threshold element results.

CONCLUSION

The intention of the author of this report was to show the progessive development of the adaptive threshold element. A brief review of the learning system philosophy has been presented first. This was followed by a short description of the equipment already available at the University of Ottawa with a summary of the experiments previously performed. The need of a self-adaptive device was then pointed out. Different approaches were considered and the reasons for selecting the present one were outlined. Steps of the development were then described.

The idea of utilizing a Hall element inserted in the air gap of a ferromagnetic square loop material has undoubtedly been shown as one of the right and promising approaches. However, before the proposed scheme may become practical, there are many improvements to be incorporated. A survey of all the available ferrite toroids should be made in order to determine the best prospects for the present use. This, of course, would require a close and efficient cooperation with the suppliers. The author, unfortunately, cannot claim to have received such cooperation from manufacturers. However, if the goals were carefully explained (which the present author did not do), probably a better cooperation could be established.

The tolerances in the dimensions of the Hall element have been rather poor up to now. A 25% margin has been noticed

in certain cases and this surely does not help. It is believed that the manufacturer could certainly improve this situation.

The delay and separator have not been built in terms of hardware. However, the use of an R-C network should produce the necessary delay while the separator could be designed around a silicon controlled rectifier.

-BIBLIOGRAPHY-

1. F.H. George, "Machines and the Brain", Science, Vol. 127, No. 3309, pp. 1269-1274, May 1958.

2. D.O. Hebb, "Organization of Behavior", John Wiley and Sons, New York, N.Y., 1949.

3. O.H. Mowrer, "Learning Theory and Behavior", John Wiley and Sons, New York, N.Y., 1960.

4. F. Rosenblatt, "Principles of Neurodynamics - Perceptrons and the Theory of Brain Mechanisms", Cornell Aeronautical Lab., Buffalo, N.Y., Rept. No. VG-1196-G-8, March, 1961.

5. R.J. Scott, "Construction of a Neuron Model", IRE Transactions on Bio-Medical Electronics, pp. 198-202, July, 1961.

6. L.D. Harmon and R.M. Wolfe, "An Electronic Model of a Nerve Cell", Semiconductor Products, Vol. 2, No. 8, pp. 36-40, August, 1959.

7. M.B. Herscher, T.B. Martin, E.P. McGrogan and F.L. Putzrath, "Neurons and Neural Networks", R.C.A. Engineer, Vol. 8, No. 1 pp. 24-28, June-July, 1962.

8. O.Boshko, G.S. Glinski and J. Therrien, "Simulation of Learning Processes", Conference Paper 61-320, presented at the AIEE Winter General Meeting, New York, N.Y., February, 1961.

9. G.S. Glinski and J. Therrien, "Direct Experimentation with Adaptive Digital Networks", Conference Paper, presented at the IRE Canadian Electronics Conference, Toronto, Ont., Can., October, 1961.

10. F. Rosenblatt, "The Perceptron - A Theory of Statistical Separability in Cognitive Systems", Cornell Aeronautical Lab., Buffalo, N.Y., Rept. No. VG-1196-G-1, January, 1958.

11. B.G. Farley and W.A. Clark, "Activity in Networks of Neuron-Like Elements", Information Theory, Fourth London Symposium, Ed. by C. Cherry, pp. 242-248, Butterworths, 1961.

12. J.A. Rajchman, "Computer Memories, a Survey of the State-of-the-Art", Proc. IRE, Vol. 49, pp. 104-127, January, 1961.

13. B. Widrow, "Generalization and Information Storage in Networks of Adaline Neurons", Self-Organizing Systems 1962, M.C. Yovits, G.T. Jacobi and G.T. Goldstein Editors, Spartan Books, Washington, D.C., 1962.

14. E.B. Carne, "Self-Organizing Models - Theory and Techniques", Proc. National Aerospace Electronics Conference (NAECON), 1962.

15. J.K. Hawkins, "Self-Organizing Systems - a Review and Commentary", Proc. IRE, Vol. 49, pp. 31-48, January, 1961.

16. B. Widrow, W.H. Pierce and J.B. Angell, "Birth, Life and Death in Microelectronic Systems", IRE Trans. on Military Electronics, pp. 191-201, July, 1961.

17. M. Minsky and O.G. Selfridge, "Learning in Random Nets", Information Theory, Fourth London Symposium, Ed. by C. Cherry, pp. 335-347, Butterworths, 1961.

18. D.G. Willis, "Plastic Neurons as Memory Elements", Proc. International Conference on Information Processing, pp. 291-297, UNESCO, Paris, June 1959.

19. J.K. Hawkins, C.J. Munsey and R.A. Stafford, "A Magnetic Integrator for the Perceptron Program", Summary Report, Aeronutronic, Newport Beach, Cal., Publication No. U-1405, Sept., 1961.

20. J.K. Hawkins and C.J. Munsey, "A Magnetic Integrator for the Perceptron Program", Annual Summary Report, Aeronutronic, Newport Beach, Cal., Publication No. U-603, July, 1960.

21. B. Widrow, "An Adaptive Adaline Neuron Using Chemical Memistors", Stanford University, Electronics Lab., Cal., TR-1553-2, Nonr 225 (24), NR-373,360, October, 1960.

22. G. Nagy, "Analogue Memory Mechanisms for Neural Nets", Cognitive Systems Research Program, Cornell University, Ithaca, N.Y., Rept. No. 3, August, 1962.

23. J.A. Rajchman and A.W. Lo, "The Transfluxor", Proc. IRE, Vol. 44, pp. 321-332, March, 1956.

24. C.L. Coates and E.A. Fisch, "Design of a Solid State Neuron Circuit", General Electric, Electronics Lab., Rept. No. R-60-ELS-39, Syracuse, N.Y., March, 1960.

25. E.H. Hall, "On the New Action of Magnetism on a Permanent Electric Current", Philosophical Magazine, Vol. 10, pp. 301-328, November, 1880.

26. J. Vermot-Gaud, "Etude d'une Application de l'Effet Hall - la Réalisation d'Elements de Circuits Logiques", Annales des Télécommunications, Vol. 6, pp. 133-151, May-June, 1961.

27. G.S. Glinski and P.A. Deschenes, "Dispositif de Mémoire Utilisant l'Effet Hall", Conference Paper presented at the annual symposium of the Acfas, Montreal, P.Q., Can., November 1962.

28. J. Wylen, "Pulse Response Characteristics of Rectangular-Hysteresis-Loop Ferromagnetic Materials", Trans. of the AIEE, Part 1. Communications and Electronics, Vol. 72, pp. 648-656, November, 1953.

29. J.D. Freeman, "New Idea in Counting", Electronics, Vol. 35, No. 24, pp. 40-43, June, 1962.

30. J.R. Bacon and G.H. Barnes, "Quantized Flux Counter", IRE Wescon Convention Record, Part 4, pp. 246-250, 1957.

31. R.M. Bozorth, "Ferromagnetism", D. Van Nostrand, Inc., Princeton, New Jersey, 1956.

32. C. Kittel, "Introduction to Solid State Physics", John Wiley and Sons, New York, N.Y., 1961.

33. H.C. Roters, "Electromagnetic Devices", John Wiley and Sons, New York, N.Y., 1955.

34. S.S. Attwood, "Electric and Magnetic Fields", John Wiley and Sons, New York, N.Y., 1956

35. W.R. Chynoweth and al., "Solid States Magnetic and Dielectric Devices", John Wiley and Sons, New York, N.Y., 1959.

36. E.E. Staff, MIT, "Magnetic Circuits and Transformers", The Technology Press, Massachusetts Institute of Technology, John Wiley and Sons, New York, N.Y., 1958.

37. C.D. Owens, "Analysis of Measurements on Magnetic Ferrites", Proc. IRE, Vol. 41, pp. 359-365, March 1953.

38. J.J. Went and E.W. Gorter, "The Magnetic and Electrical Properties of Ferroxcube Materials", Philips Technical Review, Vol. 13, No. 7, pp. 181-208, January, 1952.

39. M.A. Vassiliev, "Materiaux Magnétiques à Mémoire, Alliages et Ferrites Spéciaux", L'Onde Electrique, Vol. 35, No. 340, pp. 672-681, July 1955.

VITA

Name : Deschenes Pierre A.

Born : Shawinigan, P.Q., September 5, 1934

Educated :

Primary : Ecole St-Georges, Shawinigan, P.Q.

Secondary : Séminaire de Joliette, Joliette, P.Q.

University : Université de Montréal, Montréal, P.Q.

Course : Arts

Degree : B.A., 1955

University : McGill University, Montreal, P.Q.

Course : Electrical Engineering

Degree : B. Eng. 1960